arXiv:1511.03998v1 [quant-ph] 12 Nov 2015

Multipartite Entanglement Accumulation in Quantum States: Localizable Generalized Geometric Measure

Debasis Sadhukhan, Sudipto Singha Roy, Amit Kumar Pal, Debraj Rakshit, Aditi Sen(De), and Ujjwal Sen
Harish-Chanda Research Institute, Chhatnag Road, Jhunsi, Allahabad - 211019, India

Multiparty quantum states are useful for a variety of quantum information and computation protocols. We define a multiparty entanglement measure based on local measurements on the multiparty quantum state, and an entanglement measure averaged on the post-measurement ensemble. Using the generalized geometric measure as the measure of multipartite entanglement for the ensemble, we demonstrate, in the case of several well-known classes of multipartite pure states, that the localized multipartite entanglement can exceed the entanglement present in the original state. We also show that measurement over multiple parties may be beneficial in enhancing localizable multipartite entanglement. We point out that, compared to the generalized geometric measure, localizable generalized geometric measure works better in signaling quantum critical phenomena occurring in well-known quantum spin models even when considerable finite-size effect is present in the system.

I. INTRODUCTION

Emergence of multipartite entanglement [1] as a crucial ingredient in several information processing tasks like measurement-based quantum computation [2], quantum dense coding [3–5], and quantum cryptography [6–8] has emphasized the importance of quantifying entanglement in multipartite systems. Multipartite entanglement has been proven essential also in detecting cooperative phenomena such as quantum phase transitions [9, 10], and to explain transport properties in photosynthetic complexes [11] (see [12–14] for reviews). In this respect, it has also been pointed out that multipartite entanglement can be necessary to detect some cooperative phenomena, which are not clearly signaled by bipartite measures [15]. The growing interest for estimating multipartite entanglement in many-body systems is also sustained by impressive experimental advances towards creating entangled particles in laboratories in various substrates, *e.g.*, trapped ions [16], photons [17], superconducting materials [18], nuclear magnetic resonances [19], and optical lattices [20] (see also [21]). However, despite considerable attempts, progress in developing measures of multipartite entanglement has been limited [1, 10, 22–31].

An interesting utility of multipartite quantum states is the measurement based quantum computation [2], where quantum gates are implemented by solely performing suitable measurements on different local parts of a previously prepared quantum state of a number of parties, eg., on a lattice. In a different situation, one may consider performing measurements on some parts of a multiparty quantum state, so that the remaining parties share a useful quantum state. A particularly important example is provided by the Greenberger-Horne-Zeilinger (GHZ) state [32], given by $|\psi\rangle = (|0\rangle^{\otimes N} + |1\rangle^{\otimes N})/\sqrt{2}$. Tracing out m qubits from $|\psi\rangle$, where $m < N-1$, leads to a separable state with vanishing entanglement, while performing local measurements over the m parties, one obtains an ensemble of pure states conditioned to the measurement outcomes, which has non-zero entanglement. Such protocols encourages one to consider a general scenario where an N-party quantum state, ρ_N, is measured at a certain number of parties, to obtain an ensemble of a lower number of parties, where no measurement was carried out, with the measurements being so chosen that the average entanglement, according to a predecided measure, of the pre-measurement ensemble is minimized. Such entanglement accumulation scheme have been previously used to define entanglement measures [33–36], where it was usual to choose the number of unmeasured parties as two. Here we go beyond the regime, where the the number of parties in the post-measurement ensemble is more than two.

In this paper, we introduce a localizable multipartite entanglement (LME) measure, in terms of the geometric measures of entanglement [10, 27, 30], and discuss its various properties. Specifically, we prove that the localizable multipartite entanglement measure is invariant under local unitary transformations, and show that it is bounded above by any upper bound of its parent multiparty entanglement. Note that the concept of LME requires the knowledge of another multiparty entanglement measure, and due to the compact computational form of multiparty entanglement, as quantified by the generalized geometric measure (GGM) [10, 27, 30], we restrict ourselves to the cases in which the GGM is identified with the latter measure. We call the corresponding quantity as the localizable GGM (LGGM). For arbitrary number of qubits, we analytically find the exact expression of LGGM for several classes of multipartite states which include the generalized GHZ (gGHZ) state [32], generalized W (gW) state [35, 37, 38], and Dicke states with different excitations [39–41], when measurement is restricted to a single qubit. Interestingly, we find that in the case of gGHZ state, LGGM coincides with the GGM of the original state. On the other hand, for gW state, local measurement helps to accumulate higher multipartite entanglement in the lower number of qubits, as compared to the content of multipartite entanglement of the original state, showing qualitatively distinct behavior than the gGHZ state. Moreover, we prove that the value of LGGM over two qubits in the case of an arbitrary three-qubit pure state is always lower bounded by the value of the geometric measure of the original state, while no such bound exists when higher number of qubits are involved.

For specific classes of four- and five-qubit states, we show that local measurement on two parties may help to increase LGGM, as compared to the same with only single-qubit measurement. Extensive numerical simulations seems to imply that such observation holds for almost all four- and five-qubit states. Such investigations lead to a natural question whether LGGM is more useful than the other multipartite entanglement measures of the original state. For detecting the quantum phase transition (QPT) [42] of the quantum Ising model in a transverse field [43], we

observe that the system approaches to the quantum critical point much faster when LGGM is used as the observable compared to its counterpart of the original state. We use finite-size calculations to analyze the relative speed of the approach to the critical point. Besides, we find that LGGM faithfully signals the Kosterlitz-Thouless (KT) transition of the XXZ model [44–47].

The paper is organized as follows. Sec. II contains the formal definition of LME using geometric measures as the quantifier. It also describes various properties of LME. Sec. III describes the results regarding single-qubit measurement in the case of several well-known examples of multiqubit states, such as the generalized GHZ state, the generalized W state, and the N-qubit symmetric states. The effect of measurement over more than one qubit on the value of LME, along with specific examples in the case of four- and five-qubit systems, is discussed in Sec. IV. The numerical results regarding arbitrary three-, four-, and five-qubit pure states are presented in Sec. V. Sec. VI deals with the study of the behavior of LME in well-known quantum spin models. Sec. VII contains the concluding remarks.

II. LOCALIZABLE MULTIPARTITE ENTANGLEMENT

In this section, we formally introduce the LME, and discuss its properties.

A. Definition

The LME of a multiparty pure state can be defined as the maximum average multipartite entanglement that can be concentrated over a certain specified set of parties in the system by performing local measurements over the rest of the parties. Let us consider a pure state $|\Phi_N\rangle$, which describes a multipartite system consisting of N parties distinguished by the index $i = 1, 2, \cdots N$. For simplicity, while defining the LME, we consider that the dimension of Hilbert space of each of the parties is same, i.e., $d_i = d$, $i = 1, \cdots, N$. However, a more generalized definition using different dimensions for different parties can also be given.

Let us consider local quantum measurements performed by any m parties on the N-party state, $|\Phi_N\rangle$. Let $\mathbf{r}$ be the set of positions of the measured qubits, given by $\mathbf{r} = \{r_j\}, j = 1, \cdots, m$, where $r_j \in \{1, 2, \cdots, N\}$. The local measurements lead to a post-measurement outcome ensemble, $\{p^l, |\Psi_N^l\rangle\}$, of pure states. The index l denotes the running index of the measurement outcomes, and runs over the joint Hilbert space of the measured parties having dimension d^m. Here, p^l is the probability of obtaining the state $|\Psi_N^l\rangle = M^l|\Phi_N\rangle$, with M^l being the corresponding measurement operator, and $\sum_{l=1}^{d^m} p^l = 1$. The LME for the multipartite state $|\Phi_N\rangle$, for local measurements at $\mathbf{r}$, can be defined as

$$E_{L,\mathcal{E}}^{n,\mathbf{r}}(|\Phi_N\rangle) = \sup_{\mathcal{M}} \sum_{l=1}^{d^m} p^l \mathcal{E}\left(|\psi_n^l\rangle\right), \tag{1}$$

where $\mathcal{M} \equiv \{M^l\}$ is a complete set of measurement operators on the d^m-dimensional Hilbert space, and $\mathcal{E}(|\psi\rangle)$ is an arbitrary multipartite entanglement measure for the state $|\psi\rangle$. Here, $n = N - m$ $(n \leq N - 1)$, and is currently redundant in the notation. Its use will become clear once we reach Eq. (3). We will also assume that $n \geq 2$, although the formalism adopted here can be generalized to the case of $n = 1$ also. The state $|\psi_n^l\rangle$ corresponding to the N-party state $|\Psi_N^l\rangle$, for a fixed $\mathbf{r}$ and a fixed measurement outcome l, is obtained by tracing out the m parties in which local measurements are performed. The supremum is taken over all complete sets of measurement operators, $\mathcal{M}$.

It is important to note here that the conceptualization of an LME depends on the understanding of another measure of multiparty entanglement of a lower number of parties. this latter measure is in some sense acting as a "seed measure" for the LME. To define LME, one may consider measurement protocols corresponding to either projective measurements (PV) without classical communication between the parties, or positive operator valued measures (POVMs) without classical communication between the parties, or general local operations and classical communication (LOCC). In the last case, the classical communication (CC) is among the m parties over which the local operations are performed. It is clear that

$$E_{L,\mathcal{E}}^{n,\mathbf{r}}|_{\text{PV}} \leq E_{L,\mathcal{E}}^{n,\mathbf{r}}|_{\text{POVM}} \leq E_{L,\mathcal{E}}^{n,\mathbf{r}}|_{\text{LOCC}}, \tag{2}$$

for a fixed multipartite state, $|\Phi_N\rangle$, a fixed set of measured parties, $\mathbf{r}$, and a chosen multiparty entanglement measure, $\mathcal{E}$.

One must note here that for a fixed initial multipartite state $|\Phi_N\rangle$, the value of LME depends on two factors: **(i)** the multipartite entanglement measure $\mathcal{E}$ (the seed measure), and **(ii)** the set $\mathbf{r}$, i.e., the choice of m parties over which local measurements are performed. Before discussing the choice of $\mathcal{E}$, let us briefly consider the dependence of LME over the set $\mathbf{r}$ that is inherent in the definition. For an N-partite system with local measurements at m parties, a set $\mathbf{R} = \{\mathbf{r}_\alpha\}$, $\alpha = 1, 2, .., \binom{N}{m}$, of all possible choices of $\mathbf{r}$ exists, thereby allowing $\binom{N}{m}$ number of values of LME, $E_{L,\mathcal{E}}^{n,\mathbf{r}_\alpha}$. Therefore, the LME, $E_{L,\mathcal{E}}^{n,\mathbf{r}_\alpha}$, is "local" in the sense that it changes with the choice of the set $\mathbf{r}_\alpha$. In light of this fact, one can also define a "global" value of the LME for a multipartite state with fixed values of N and m as

$$E_{GL,\mathcal{E}}^{n} = \max_{\mathbf{R}} \{E_{L,\mathcal{E}}^{n,\mathbf{r}_\alpha}\}. \tag{3}$$

Note that if the initial state $|\Phi_N\rangle$ is a symmetric state, such maximization over $\mathbf{R}$ is not required. Note also that the relative positions of the parties labeled by "$\mathbf{r}_\alpha$", for a specific α, with respect to each other as well as the rest of the parties does not affect the value of LME. From now on, without any loss of generality, we assume that the measurements are performed at $r_j = j$, $j = 1, 2, \cdots, m$, while $|\psi_n^l\rangle$ denotes the state of the remaining n parties.

We can extend this definition to an arbitrary mixed state when the input state is an N-party state $\varrho_{1,2,\cdots,N}$, and the measurement is performed on any m parties. The problem in this case remains with the choice of $\mathcal{E}$, which is possible to compute for a given multiparty state. Such multiparty quantum correlation measures are rare.

Multipartite entanglement measures

Although the notion of entanglement measures in multipartite systems is an active field of research, the number of such

computable measures is still limited. In principle, an LME can be defined for any one of the known candidates for multipartite entanglement measure being used as the seed measure, such as relative entropy of entanglement [22], global entanglement [23], and other multipartite measures [1, 24]. However, in the present study, we focus on geometric measures (GM) of entanglement [1, 9, 10, 25–28].

The geometric measure of entanglement of an N-partite state $|\tilde{\Psi}_N\rangle$, is defined as

$$G_K(|\tilde{\Psi}_N\rangle) = 1 - \max_{\mathcal{S}_K} |\langle \tilde{\Phi}_N^K | \tilde{\Psi}_N \rangle|^2, \tag{4}$$

where K ($2 \leq K \leq N$) is an integer denoting the number of product state partitions into which the N-partite state $|\tilde{\Phi}_N^K\rangle$ can be divided [1, 9, 10, 25–28]. The distance of the state $|\tilde{\Psi}_N\rangle$ is minimized over the set, $\mathcal{S}_K$, of all K-separable pure states, $|\tilde{\Phi}_N^K\rangle$, and we refer to this measure as "K-separability based GM" (K-GM). For example, $K = N$ corresponds to a fully separable state $|\tilde{\Phi}_N^N\rangle \equiv \bigotimes_{i=1}^N |\tilde{\phi}_i\rangle$, leading to the original definition of GM [25, 28]. On the other hand, GGM is obtained for $K = 2$ [10, 27], the other extremum of K-GM, which we denote by $\mathcal{G}(|\tilde{\Psi}_N\rangle)$. The optimization in the definition of $\mathcal{G}(|\tilde{\Psi}_N\rangle)$ can be performed by using the maximization of the Schmidt coefficients across all possible bipartitions of $|\tilde{\Psi}_N\rangle$, leading to the simplified version of GGM [10], given by

$$\mathcal{G}(|\tilde{\psi}_N\rangle) = 1 - \max_{\mathcal{S}_{\mathcal{A}:\mathcal{B}}} \{\lambda^2_{\mathcal{A}:\mathcal{B}}\}. \tag{5}$$

Here, $\lambda_{\mathcal{A}:\mathcal{B}}$ is the maximum Schmidt coefficient of $|\tilde{\Psi}_N\rangle$, the maximum being taken over the set, $\mathcal{S}_{\mathcal{A}:\mathcal{B}}$, of all arbitrary $\mathcal{A} : \mathcal{B}$ bipartitions such that $\mathcal{A} \cup \mathcal{B} = \{1, 2, \cdots, N\}$, and $\mathcal{A} \cap \mathcal{B} = \mathbf{\Phi}$, the null set. The above expression allows one to compute GGM of a multiparty pure state in arbitrary dimensions and for arbitrary number of parties.

B. Properties

We now prove several properties of LME. We use K-GM as the multipartite entanglement measure, and local projective measurements, in which case, Eq. (1) reads

$$E_L^{n,\mathbf{r}_\alpha}(|\Phi_N\rangle) = \sup_{\mathcal{P}} \sum_{l=1}^{d^m} p^l G_K\left(|\psi_n^l\rangle\right), \tag{6}$$

where $\mathcal{P} \equiv \{P^l\}$ denotes a complete set of local projectors acting on the parties distinguished by $\mathbf{r}_\alpha$. From now onward, we discard the index $\mathcal{E}$. We start by looking into the bounds of the measure, which leads us to the following theorem.

Theorem 1. *For an arbitrary state $|\Phi_N\rangle$ describing a quantum system of N parties, $0 \leq E_L^{n,\mathbf{r}_\alpha} \leq g$, where $G_K \leq g$.*

Corollary 1 follows directly from Theorem 1, and the definition of E_{GL}^n (Eq. (3)).

Corollary 1.1 For an arbitrary state $|\Phi_N\rangle$ describing a quantum system of N parties, $0 \leq E_{GL}^n \leq g$, where $G_K \leq g$.

Note that for $K = 2$, $G_K \equiv \mathcal{G}$ for an N-qubit system, and the above property implies $E_L^{n,\mathbf{r}_\alpha} \leq 1/2$, since $\mathcal{G} \leq 1/2$. Our next theorem is on the effect of local unitary operations on LME.

Theorem 2. *$E_L^{n,\mathbf{r}_\alpha}$ remains invariant under local unitary transformations.*

To determine the criteria for vanishing $E_L^{n,\mathbf{r}_\alpha}$, we intend to characterize the set of multipartite states, $\{|\Phi_N\rangle\}$, for which $E_L^{n,\mathbf{r}_\alpha} = 0$. We first consider the following theorem.

Theorem 3. *For a K-separability based GM, a non-zero value of $E_L^{n,\mathbf{r}_\alpha}$ for an N-partite pure state, $|\Phi_N\rangle$, is possible with $n = N - m$, m being the number of parties in which measurement is performed, only when the separability, M, of the original state is such that $1 \leq M \leq K + m - 1$.*

Proof. To prove the above theorem, let us first assume that the N-partite system is composed of two partitions denoted by A, and B. The first one consists of the m parties over which local measurements are performed, while the rest $n = N - m$ parties construct the partition B. For the value of $E_L^{n,\mathbf{r}_\alpha}$ to be non-zero, at least one of the states, $\{\psi_n^l\}$, of the post-measurement ensemble consisting of d^m states must not be K-separable, so that $G_K(|\psi_n^l\rangle) \neq 0$. This implies that the state $|\psi_n^l\rangle$ is allowed to be K'-separable, where $1 \leq K' \leq K - 1$. Moreover, irrespective of whether the partitions A and B share entanglement amongst each other, the possible separability of the partition A consisting of m parties dictates that the original state, $|\Phi_N\rangle$, is allowed to be $(K' + j)$-separable, where $1 \leq j \leq m$. Combining these two results, one obtains the allowed range of M as 1 to $K + m - 1$. ■

All the characteristics of LME discussed above remains unchanged if K-GM is replaced by GGM as the genuine multipartite entanglement measure. Motivated by the computability of GGM, we discuss the properties of several well-known three-, four-, and N-qubit systems using LGGM as the LME, i.e., using the GGM for $\mathcal{E}$, and establish its relations with the well known multipartite quantum correlation measures.

III. SINGLE-QUBIT MEASUREMENT: LGGM VS. GGM

Let us consider an N-party pure state in $(\mathbb{C}^2)^{\otimes N}$. The local projective measurement, $\mathcal{P}$, on a qubit j ($j = 1, 2, \cdots, N$), can be represented by a complete set of rank-1 projectors, $\{\Pi_j^l\}$, such that $\Pi_j^l = |\xi_j^l\rangle\langle\xi_j^l| \otimes \mathbb{I}_{N-1}$, $l = 1, 2$, given by

$$\begin{aligned} |\xi_j^1\rangle &= c_{\theta_j/2}|0\rangle + e^{i\phi_j} s_{\theta_j/2}|1\rangle, \\ |\xi_j^2\rangle &= -s_{\theta_j/2} e^{i\phi_j}|0\rangle + c_{\theta_j/2}|1\rangle, \end{aligned} \tag{7}$$

with $0 \leq \theta_j \leq \pi$, $0 \leq \phi_j < 2\pi$, and c_x and s_x stand for $\cos x$ and $\sin x$ respectively. Here, $\mathbb{I}_{N-1}$ is the identity operator in the Hilbert space of the $N - 1$ qubits, and $\{|0\rangle, |1\rangle\}$ is the computational basis in the qubit Hilbert space. Note that Π_j^l are of rank one only, when all but the j^{th} qubit are traced out. In this representation, the supremum involved in the definition of LME is obtained by a performing a maximization over the space of the real parameters, (θ_j, ϕ_j). If local measurements are performed over a collection of qubits denoted by $\mathbf{r} \equiv \{r_j\}$, $j = 1, 2, \cdots, m$ with $m > 1$, the supremum has to be obtained over a total of $2m$ real parameters, $(\theta_{r_j}, \phi_{r_j})$.

Now, we calculate the LGGM for a number of well-known pure states with arbitrary number of parties, using GGM as the multipartite measure of entanglement.

A. Generalized GHZ state

The first example is the N-qubit generalized GHZ state for which we can analytically find the exact value of LGGM for arbitrary number of qubits. The state is given by [32]

$$|GHZ_N\rangle_g = a_1|0\rangle^{\otimes N} + a_2|1\rangle^{\otimes N}, \tag{8}$$

where a_1 and a_2 are complex numbers with $|a_1|^2 + |a_2|^2 = 1$. Without any loss of generality, let us assume that $|a_1|^2 \geq \frac{1}{2} \geq |a_2|^2$. Let us first consider the case of $m = 1$. Therefore, Eq. (1) can be presented in a simpler form, as

$$E_L^r = \sup_{\mathcal{P}} \sum_{l=1}^{2} p^l \mathcal{G}(|\psi_{N-1}^l\rangle). \tag{9}$$

Note here that in Eq. (9), we have discarded the superscript n since it has a constant value $n = N - 1$ in the present case. We also replace $\mathbf{r}_\alpha$ with r since the position index, r, of the qubit over which the local projective measurement is performed, can now have N possible values, i.e., $r = 1, 2, \cdots, N$. As $|GHZ_N\rangle_g$ is symmetric under swapping of parties, we have $E_L^r = E_L$ for $r = 1, 2, \cdots, N$. Here and in the rest of the paper, unless otherwise stated, we always consider local measurement over the first qubit of the system in the case of a single-qubit measurement.

Proposition I. *For the N-qubit gGHZ state, $E_L^1 = \mathcal{G}$.*

Proof. Once the rank-1 projective measurement is performed over the first qubit, an ensemble of two pure states, $\{p^l, |\Psi^l\rangle\}$, $l = 1, 2$, is obtained, where $p^l = |a_1|^2 q_1^l + |a_2|^2 q_2^l$, $|\Psi^l\rangle = |\xi_1^l\rangle \otimes |\psi^l\rangle$ for $l = 1, 2$, and $|\psi^l\rangle = (a_1 z_1^l |0\rangle^{\otimes N-1} + a_2 z_2^l |1\rangle^{\otimes N-1})/\sqrt{p^l}$. The quantities $q_{1,2}^l$ and $z_{1,2}^l$ are given by

$$\begin{aligned} q_1^l &= (\delta_{1l} c_{\theta/2}^2 + \delta_{2l} s_{\theta/2}^2), \\ q_2^l &= (\delta_{1l} s_{\theta/2}^2 + \delta_{2l} c_{\theta/2}^2), \end{aligned} \tag{10}$$

and

$$\begin{aligned} z_1^l &= \delta_{1l} c_{\theta/2} - \delta_{2l} e^{-i\phi} s_{\theta/2}, \\ z_2^l &= \delta_{1l} e^{i\phi} s_{\theta/2} + \delta_{2l} c_{\theta/2}, \end{aligned} \tag{11}$$

with δ_{kl}, $k = 1, 2$, being Kronecker delta. Note that the states $|\psi^l\rangle$ are of the form of an $(N-1)$-qubit gGHZ state. Note also that for an N-qubit gGHZ state, the local density matrix, ρ_n, of n qubits, is diagonal in the computational basis with only two non-zero elements. Hence, in the present case, the LGGM of the gGHZ state can be obtained from Eq. (9), where $\mathcal{G}(\psi_{N-1}^l) = 1 - \max\left\{|a_1|^2 q_1^l/p^l, |a_2|^2 q_2^l/p^l\right\}$ with $p^l = |a_1|^2 q_1^l + |a_2|^2 q_2^l$. Using the identity, $\max\{x, y\} + \max\{u, v\} = \max\{x+u, x+v, y+u, y+v\}$ for arbitrary values of x, y, u, and v, in Eq. (9), one obtains

$$E_L^1 = 1 - \min_\theta \left[\max\left\{|a_1|^2, s_{\theta/2}^2, c_{\theta/2}^2\right\}\right]. \tag{12}$$

In $[0, \pi]$, $c_{\theta/2}^2$ is a monotonically decreasing function whereas $s_{\theta/2}^2$ is a monotonically increasing one, and the maximum value of both the functions is unity, occurring at $\theta = 0$ for $c_{\theta/2}^2$, and $\theta = \pi$ for $s_{\theta/2}^2$. Besides, the values of both functions are equal to $1/2$ at $\theta = \pi/2$. Since $|a_1|^2 \geq 1/2 \geq |a_2|^2$, the allowed range of θ can be divided into three subregions: **(i)** $0 \leq \theta \leq \theta_1$, where $c_{\theta/2}^2 \geq |a_1|^2 \geq s_{\theta/2}^2$, **(ii)** $\theta_1 < \theta < \theta_2$, where $|a_1|^2 \geq \max\{c_{\theta/2}^2, s_{\theta/2}^2\}$, and **(iii)** $\theta_2 \leq \theta \leq \pi$, where $s_{\theta/2}^2 \geq |a_1|^2 \geq c_{\theta/2}^2$. Here, the values of θ_1 and θ_2 are obtained as solutions of the equations $c_{\theta/2}^2 = |a_1|^2$ and $s_{\theta/2}^2 = |a_1|^2$ respectively. The maximization inside the curly bracket in Eq. (12) has to be performed for a fixed value of θ, which can be chosen from any one of the three subregions, **(i)**, **(ii)**, and **(iii)**. Noticing that $\min(c_{\theta/2}^2) = |a_1|^2$ for $0 \leq \theta \leq \theta_1$, while $\min(s_{\theta/2}^2) = |a_1|^2$ in the region $\theta_2 \leq \theta \leq \pi$, from Eq. (12), one obtains $E_L^1 = |a_2|^2$. Note here that the GGM of the gGHZ state, under the assumption that $|a_1|^2 \geq \frac{1}{2} \geq |a_2|^2$, is also $|a_2|^2$, leading to $E_L^1 = \mathcal{G}$. ■

The value of LGGM remains unchanged in the case of the gGHZ state if measurement is performed over a higher number of qubits ($m > 1$). However, in subsequent discussions, we shall be providing examples of multipartite quantum states for which the situation is different.

GHZ state. As a special case of the N-qubit gGHZ state, the LGGM for the GHZ state ($a_1 = a_2 = 1/\sqrt{2}$) of N qubits can be obtained as $E_L^1 = 1/2$.

B. Generalized W state

Next, let us look into the LGGM for N-qubit gW state, given by [35, 37, 38]

$$|W_N\rangle_g = \sum_{i=1}^{N} a_i |0\rangle^{\otimes(i-1)} |1\rangle_i |0\rangle^{\otimes(N-i)}, \tag{13}$$

where $\{a_i\}$, $i = 1, 2, \cdots, N$, are complex numbers so that $\sum_{i=1}^{N} |a_i|^2 = 1$. Note that unlike the gGHZ state, the gW state is not symmetric under swapping of parties, which leads to a collection of N values of LGGM, $\{E_L^r\}$, $r = 1, 2, \cdots, N$.

For the purpose of demonstration, we start with the case of $N = 3$, where measurement is performed over qubit 1. Since the gW state is not symmetric, LGGM may depend on the choice of the measured parties. The GGM of the state, in the present case, is given by $\mathcal{G} = \min\{|a_i|^2\}$, where $i = 1, 2, 3$. The post measurement ensemble is $\{p^l = (|a_2|^2 + |a_3|^2) q_1^l + |a_1|^2 q_2^l, |\psi^l\rangle = [z_1^l (a_2|10\rangle + a_3|01\rangle) + z_2^l a_1 |00\rangle]/\sqrt{p^l}\}$, $l = 1, 2$, where $z_{1,2}^l$ and $q_{1,2}^l$ are given in Eqs. (10) and (11) respectively. One must note that the GGM of two-qubit states of the form $|\psi^l\rangle$ is invariant under an interchange of a_2 and a_3. The LGGM (Eq. (9)), in this case, is given by

$$E_L^1 = \frac{1}{2}\left(1 - \min_\theta \sum_{l=1}^{2} \sqrt{f^l(\theta)}\right), \tag{14}$$

where $f^l(\theta) = {p^l}^2 - 4|a_2|^2|a_3|^2 u^l$, and

$$u^l = \delta_{1l} c_{\theta/2}^4 + \delta_{2l} s_{\theta/2}^4. \tag{15}$$

The validity of the single qubit density matrix ρ_2^l of qubit 2, obtained from the state $|\psi^l\rangle$, demands that $f^l(\theta) \geq 0 \; \forall \; \theta$. The function $f(\theta) = \sum_{l=1}^{2} \sqrt{f^l(\theta)}$ has minimum at $\theta = 0, \pi$ in

	Ordering	$\mathbf{E_L^1}$	$\mathbf{E_L^2}$	$\mathbf{E_L^3}$	$\mathcal{G}$	Bipartition
1	$\|a_1\|^2 \geq \|a_2\|^2 \geq \|a_3\|^2$	$\|a_2\|^2$	$\|a_3\|^2$	$\|a_3\|^2$	$\|a_3\|^2$	1:23
2	$\|a_1\|^2 \geq \|a_3\|^2 \geq \|a_2\|^2$	$\|a_2\|^2$	$\|a_3\|^2$	$\|a_2\|^2$	$\|a_2\|^2$	2:13
3	$\|a_2\|^2 \geq \|a_1\|^2 \geq \|a_3\|^2$	$\|a_1\|^2$	$\|a_3\|^2$	$\|a_3\|^2$	$\|a_3\|^2$	1:23
4	$\|a_2\|^2 \geq \|a_3\|^2 \geq \|a_1\|^2$	$\|a_1\|^2$	$\|a_1\|^2$	$\|a_3\|^2$	$\|a_1\|^2$	3:12
5	$\|a_3\|^2 \geq \|a_1\|^2 \geq \|a_2\|^2$	$\|a_2\|^2$	$\|a_1\|^2$	$\|a_2\|^2$	$\|a_2\|^2$	2:13
6	$\|a_3\|^2 \geq \|a_2\|^2 \geq \|a_1\|^2$	$\|a_1\|^2$	$\|a_1\|^2$	$\|a_2\|^2$	$\|a_1\|^2$	2:13

TABLE I. Different orderings of $\{|a_1|^2, |a_2|^2, |a_3|^2\}$ and corresponding values of E_L^r ($r = 1, 2, 3$), and $\mathcal{G}$ in the case of three-qubit gW state. For all orderings, $E_L^1 \geq \mathcal{G}$. The last column shows the bipartition from which the maximum Schmidt coefficient is obtained.

the interval $0 < \theta < \pi$, while having a maximum at $\theta = \pi/2$. Hence the optimization in LGGM, in this case, is achieved when measurement is performed in the $\{|0\rangle, |1\rangle\}$ basis. From Eq. (14), it can be shown that $E_L^1 = \min\{|a_2|^2, |a_3|^2\}$. In general, for the local projective measurement being performed on the qubit r, $E_L^r = \min\{|a_j|^2, |a_k|^2\}$, where $r \neq j \neq k$, and $r, j, k \in \{1, 2, 3\}$. This leads us to a non-trivial lower bound of LGGM for the tripartite gW state, which is invariant to a change in the choice of the measured qubit, as given by the following proposition.

Proposition II. *For an arbitrary three-qubit gW state, $E_L^r \geq \mathcal{G}$ for all values of r.*

Proof. We first consider $r = 1$. Let us first assume $|a_1|^2 \geq |a_2|^2 \geq |a_3|^2$, which leads to $\mathcal{G} = \min\{|a_j|^2\}$, $j = 2, 3$. Assuming other orderings and considering all the cases, we obtain $\mathcal{G} = \min\{|a_i|^2\}$, $i = 1, 2, 3$. If $|a_i|^2 \in \{|a_2|^2, |a_3|^2\}$, then $E_L^1 = \mathcal{G}$. Else, $\mathcal{G} = |a_1|^2$, implying $E_L^1 = \min\{|a_2|^2, |a_3|^2\} \geq \mathcal{G}$. Similar proofs hold when $r = 2, 3$. ■

The following corollary regarding the lower bound of the "global" LGGM, as defined in Eq. (3), can be obtained directly from Proposition II.

Corollary II.1. For the tripartite gW state, the global LGGM, $E_{GL} \geq \mathcal{G}$.

In the case of N-qubit gW states with $N > 3$, the situation is more involved. The difficulty in determining the values of GGM of the states $|\psi^l\rangle$ in the post-measurement ensemble, which now correspond to $N-1$ qubits or less, makes analytical optimization of LGGM rather difficult. However, motivated by the Proposition II, we intend to check whether such a lower bound of LGGM exists if one considers an N-qubit gW state, when measurement is performed only on a single qubit. This leads us to the following proposition.

Proposition III. *For an arbitrary gW state of N-qubits, $E_L^r \geq \mathcal{G}$ for all values of r, provided measurement is performed only on a single qubit.*

Proof. As in the case of three-qubit systems, here also we start from the case $r = 1$. The GGM of the state $|W_N\rangle_g$ can be obtained as $\mathcal{G} = 1 - \max\{\lambda_n^{max}\}$, where λ_n^{max} is the maximum eigenvalue of all possible n-qubit reduced density matrices, $\rho_n^{\mathbf{s}}$, where $1 \leq n \leq N/2$ ($1 \leq n \leq (N-1)/2$) for even (odd) N. Here, "$\mathbf{s}$" denotes the set of all possible indices $\{s_j\}$, $j = 1, \cdots, n$, that represents the positions of the n qubits with $s_j \in \{1, 2, \cdots, N\}$. The density matrices, $\rho_n^{\mathbf{s}}$, can be written as

$$\rho_n^{\mathbf{s}} = P\left[\sum_{j=1}^{n} a_{s_j} |0\rangle^{\otimes(j-1)} |1\rangle_j |0\rangle^{\otimes(N-j)}\right] + \sum_{\substack{k=1 \\ k \notin \mathbf{s}}}^{N} |a_k|^2 P[|0\rangle^{\otimes n}], \tag{16}$$

where $P[|a\rangle] = |a\rangle\langle a|$. From Eq. (16), it is clear that the maximal eigenvalue is obtained from the case $n = 1$, and from the single qubit density matrix for which $|a_{s_1}|^2 = \min\{|a_i|^2\}$, $i = 1, 2, \cdots, N$, leading to $\mathcal{G} = |a_{s_1}|^2$.

To determine the LGGM, we first consider a measurement in the computational basis, $\{|0\rangle, |1\rangle\}$. A measurement over the first qubit in this basis leads to a product state, $|0\rangle^{\otimes(N-1)}$, with probability $p_0 = |a_1|^2$, and a pure state $|\Phi^{N-1}\rangle$, with probability $\sum_{i=2}^{N} |a_i|^2$, which can be identified as an $(N-1)$-qubit gW state. From the above discussion, $\mathcal{G}(|\Phi^{N-1}\rangle) = |a_j|^2 / \sum_{i=2}^{N} |a_i|^2$, where $|a_j|^2 = \min\{|a_i|^2\}$, $i = 2, 3, \cdots, N$. The definition of LGGM implies $E_{L,0}^1 = |a_j|^2$, where the subscript "0" indicates that the measurement is performed in the basis $\{|0\rangle, |1\rangle\}$. Clearly, $|a_j|^2 \geq |a_{s_1}|^2 \equiv \mathcal{G}$. Since the definition of LGGM involves a maximization over the complete set of projective measurements, $E_L^1 \geq E_{L,0}^1 \geq \mathcal{G}$. Similarly, one can prove for the cases $r = 2, 3, \cdots, N$, and hence the proof. ■

Our numerical analysis suggests that irrespective of the value of N, the maximization involved in LGGM for the gW states, is obtained when the local projective measurement is performed in the computational basis $\{|0\rangle, |1\rangle\}$, implying $E_L^r = E_{L,0}^r$, $r = 1, 2, \cdots, N$. Use of this information takes us to the following observation directly from Proposition III.

Observation. For an N-qubit gW state, $E_L^r \geq \mathcal{G}$ if the value of $\mathcal{G}$ is obtained from r:rest bipartition, while in all other cases, $E_L^r = \mathcal{G}$.

We demonstrate the implications of the above observation in Table I, where the E_L^r of three-qubit gW states in different cases (as distinguished by the different orderings of the $|a_i|^2$), are tabulated along with their GGMs. Note that the global LGGM, E_{GL}, is obtained when local projective measurement is performed on the qubit r so that the maximum Schmidt coefficient is obtained from the bipartition r:rest, as presented in the last column. From the table, it is clear that the value of $E_L^{r'}$, when the r':rest bipartition does not provide the maximal Schmidt coefficient, is always equal to the GGM of the three-qubit gW state, which is in agreement with the observation. We shall be investigating this issue, and its possible generalization, while discussing the LGGM of

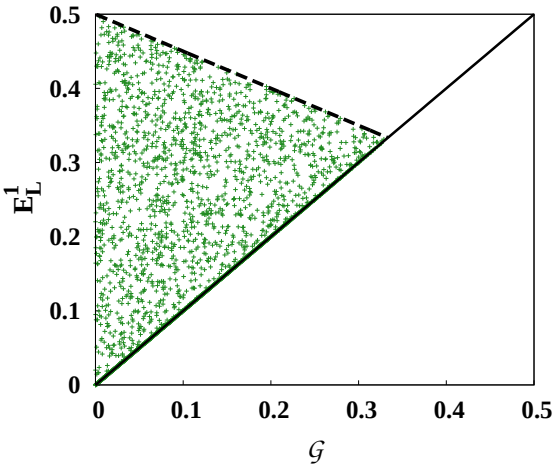

FIG. 1. (Color online.) Plot of E_L^1 vs. $\mathcal{G}$ for three-qubit gW states. To obtain the scatter diagram, 10^5 three-qubit gW states are generated Haar-uniformly. The solid line represents the line $E_L^1 = \mathcal{G}$, while the dashed line correspond to $2E_L^1 + \mathcal{G} = 1$. All quantities plotted are dimensionless.

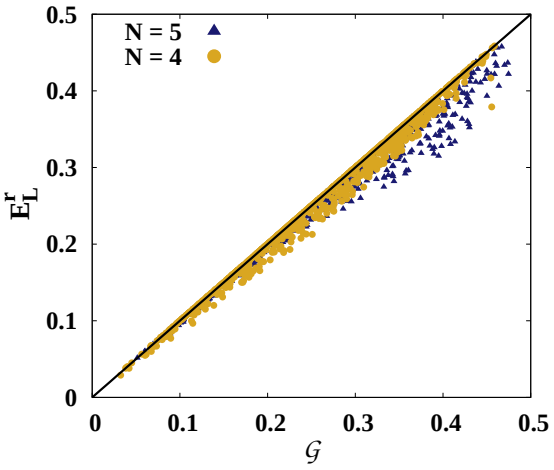

FIG. 2. (Color online.) Plot of E_L^1 vs. $\mathcal{G}$ in the case of Haar-uniformly generated generalized superposition of Dicke states, as given in Eq. (22). To obtain the scatter diagram, 10^5 states of the form $|D_g^N\rangle$ are generated Haar-uniformly for each of the cases $N = 4$ and $N = 5$. All quantities plotted are dimensionless.

arbitrary three-qubit pure states, in Sec. V A.

Considering that LGGM of the N-qubit gW state is maximized when measurement is performed in $\{|0\rangle, |1\rangle\}$, an upper bound for E_L^r of the state $|W_N\rangle_g$ can also be proved, as given in Proposition IV.

Proposition IV. *For an arbitrary N-qubit gW state, E_L^r, for all values of r, is bounded above by the LGGM of the gW state having the same value of $\mathcal{G}$, but with squared modulus of all the coefficients except one, denoted by $|a_i|^2$, being equal to $|a_j|^2 = (1 - |a_i|^2)/(N-1)$, where $|a_i|^2 = \min\{|a_k|^2\}$, $k = 1, 2, \cdots, N$, $j \neq i$, and $i, j \in \{1, 2, \cdots, N\}$.*

Proof. Let us consider a gW state given in Eq. (13) with the ordering $|a_1|^2 \leq |a_2|^2 \leq \cdots \leq |a_N|^2$. Assuming local projective measurement in qubit 1, $\mathcal{G} = |a_1|^2$ and $E_L^1 = |a_2|^2$. The assumed ordering suggests that $\max\{|a_2|^2\} = (1 - |a_1|^2)/(N-1)$, which corresponds to the LGGM of a gW state of the form $|\Phi\rangle = |a_1||1\rangle|0\rangle^{\otimes N-1} + \sum_{j=2}^{N} a_j |0\rangle^{\otimes(j-1)}|1\rangle_j|0\rangle^{\otimes(N-j)}$, with $\mathcal{G} = |a_1|^2$, similar to the arbitrary gW state, and $|a_j|^2 = (1 - |a_1|^2)/(N-1)$, $j = 2, 3, \cdots, N$. Since $\mathcal{G} = |a_i|^2 = \min\{|a_k|^2\}$ for an arbitrary N-qubit gW state with arbitrary ordering of $\{|a_k|^2\}$, $k = 1, 2, \cdots, N$, one can prove similar result for each possible ordering of $\{|a_k|^2\}$, when measurement over qubit 1 is assumed. The result also holds for an arbitrary position, r, of the measured qubit, when $r \in \{1, 2, \cdots, N\}$. Hence the proof. ■

Fig. 1 depicts the scatter diagram of E_L^1 vs. $\mathcal{G}$ in the case of a set of 10^5 Haar-uniformly generated three-qubit gW states. The solid line, representing $E_L^1 = \mathcal{G}$, depicts the lower bound of E_L^1 (Proposition II), while the dashed line, representing $2E_L^1 + \mathcal{G} = 1$, correspond to the upper bound given in Proposition IV. Note that all the points in the scatter diagram are enclosed by these two lines, and $\mathcal{G} = 0$.

W state. The W state, $|W\rangle$, is obtained from the gW state with $a_i = 1/\sqrt{N}$, $i = 1, 2, \cdots, N$. Evidently, the GGM and LGGM of the W state are equal to each other, having a value $1/N$.

C. Symmetric States

We now consider a special class of multipartite quantum states, the well-known "symmetric states", which remains unaltered with the permutation of parties. First, we investigate the behavior of LGGM in a special subset of symmetric states – the highly entangled N-qubit Dicke states [39, 40] – with high applicational advantages [41]. Then we comment on the general set of symmetric states, formed by the generalized superposition of the Dicke states.

1. *Dicke states*

An N-qubit Dicke state with k excitations can be represented as

$$|D_k^N\rangle = \frac{1}{\sqrt{\binom{N}{k}}} \sum_i \mathcal{P}_i \left(|0\rangle^{\otimes N-k} \otimes |1\rangle^{\otimes k}\right), \tag{17}$$

where the summation is over all possible permutations of N-qubit product states composed of $N-k$ qubits in the ground state, $|0\rangle$, and the rest k qubits in the excited state, $|1\rangle$. Note that the N-qubit W state can be identified as $|D_1^N\rangle$. The GGM of $|D_k^N\rangle$, with $N > 2$, can be obtained as [40]

$$\mathcal{G} = \begin{cases} \frac{N-2}{2(N-1)} \text{ for } k = \frac{N}{2}, \\ \frac{k}{N} \text{ for } k < \frac{N}{2}. \end{cases} \tag{18}$$

To determine E_L^r, $r = 1, \cdots, N$, of the Dicke state, one has to perform a rank-1 projective measurement on any one of the qubits. Since Dicke states are symmetric, the value of LGGM is independent of the position of the qubit over which measurement is performed, and the post measurement ensemble, $\{p^l, \psi^l\}$, is given by $p^l = A_k q_1^l + B_k q_2^l$ and $|\psi^l\rangle = \sqrt{A_k} z_1^l |D_k^{N-1}\rangle + \sqrt{B_k} z_2^l |D_{k-1}^{N-1}\rangle$, with $A_k = \binom{N-1}{k}/\binom{N}{k}$, and

$B_k = \binom{N-1}{k-1}/\binom{N}{k}$, while $q^l_{1,2}$ and $z^l_{1,2}$ being defined in Eqs. (10) and (11). To determine the LGGM of $|D^N_k\rangle$, one needs to calculate the GGM of $|\psi^l\rangle$, which, in turn, requires determination of the reduced density matrix of n qubits, $\rho^{l,\mathbf{s}}_n$, labeled with the set of indices $\mathbf{s} \equiv \{s_1, s_2, \cdots, s_n\}$. Since measurement over any single qubit of $|D^N_k\rangle$ yields an ensemble of symmetric states, the reduced density matrix, $\rho^{l,\mathbf{s}}_n$, of all possible collection of n qubits of the state $|\psi^l\rangle$, are equivalent. Therefore, discarding the index "s", ρ^l_n can be obtained from $|\psi^l\rangle$ as

$$\rho^l_n = \frac{1}{\binom{N}{k}p^l}\Big[\sum_{i=0}^{n} F^l_i P[|D^n_i\rangle] - (-1)^l \sum_{i=0}^{n-1} G_i\Big(e^{-i\phi}|D^n_{i+1}\rangle\langle D^n_i| + e^{i\phi}|D^n_i\rangle\langle D^n_{i+1}|\Big)\Big], \tag{19}$$

with $1 \le n \le N'$, where $N' = (N-2)/2$ ($N' = (N-1)/2$) when N is even (odd), and

$$F^l_i = \binom{n}{i}\left[\binom{N-n-i}{k-i}q^l_1 + \binom{N-n-i}{k-i-1}q^l_2\right]$$
$$G_i = \frac{s_\theta}{2}\binom{N-n-1}{k-i-1}\sqrt{\binom{n}{i+1}\binom{n}{i}}. \tag{20}$$

The GGM of $|\psi^l\rangle$ is given by $\mathcal{G}^l = 1 - \max\{\Lambda^l_n\}$, $n = 1, 2, \cdots, N'$, where Λ^l_n is the maximum eigenvalue of ρ^l_n.

We perform extensive numerical analysis for different values of N and k to find that irrespective of the number of qubits and the number of excitations, the optimization of LGGM for $|D^N_k\rangle$ always takes place at $\theta = 0, \phi = 0$, i.e., at the $\{|0\rangle, |1\rangle\}$ basis. The LGGM, in that case, can be obtained as explicit functions of N and k, as

$$E^r_L(\text{even } N) = \begin{cases} \frac{N-2}{2(N-1)} \text{ for } k = \frac{N}{2}, \\ \frac{k}{N} \text{ for } k < \frac{N}{2}. \end{cases}$$
$$E^r_L(\text{odd } N) = \begin{cases} \frac{k}{N} \text{ for } k < \frac{N-1}{2}, \\ \frac{N-1}{2N} - \frac{N+1}{4N(N-2)} \text{ for } k = \frac{N-1}{2}, N > 3, \\ \frac{1}{3} \text{ for } k = 1, 2 \text{ and } N = 3. \end{cases} \tag{21}$$

From Eqs. (18) and (21), it is evident that for $N > 3$, $E^r_L < \mathcal{G}$ for odd N with $k = (N \pm 1)/2$, while in all other cases, $E^r_L = \mathcal{G}$, thereby suggesting an upper bound of LGGM, given by $E^r_L \le \mathcal{G}$ for symmetric Dicke states of N qubits with k excitations provided the maximization is obtained in the computational basis.

2. *Generalized superposition of Dicke states*

The general form of N-qubit symmetric states can be constructed by making superpositions of all the Dicke states. Such a state can be written as

$$|D^N_g\rangle = \sum_{k=0}^{N} a_k |D^N_k\rangle, \tag{22}$$

with complex $\{a_k\}$ such that $\sum_{k=0}^{N} |a_k|^2 = 1$. Here, the summation index, k, denotes the possible number of excitations in a Dicke state, and can have values $0 \le k \le N$. Note here that an arbitrary state $|D^N_g\rangle$, upon rank-1 projective measurement over qubit r, $r = 1, 2, \cdots, N$, produces an ensemble of two $(N-1)$-qubit symmetric states represented by $\{p^l, |\bar{D}^{N-1}_g\rangle\}$, where $p^l = \sum_{k=1}^{N-1}\binom{N-1}{k}|\bar{z}^l_1 a_k + \bar{z}^l_2 a_{k+1}|^2$, $|\bar{D}^{N-1}_g\rangle = \frac{1}{\sqrt{p^l}}\sum_{k=1}^{N-1}(\bar{z}^l_1 a_k + \bar{z}^l_2 a_{k+1})|D^{N-1}_k\rangle$, with $\bar{z}^l_1 = \delta_{1l}c_{\theta/2} - (-1)^l\delta_{2l}e^{i\phi}s_{\theta/2}$, and $\bar{z}^l_2 = \delta_{1l}e^{-i\phi}s_{\theta/2} + \delta_{2l}c_{\theta/2}$. The difficulty in computing the GGM of an N-qubit symmetric state restricts one to calculate the LGGM of such states only numerically. Our numerical analysis suggests that in the case $N = 3$, $E^1_L = \mathcal{G}$, while the upper bound, $E^r_L \le \mathcal{G}$ holds in the case $N = 4, 5$, like in the case of Dicke states. Fig. 2 depicts the variation of E^r_L against $\mathcal{G}$ for 10^5 randomly chosen symmetric states for each of the cases $N = 4$, and 5, where the upper bound is satisfied. For $N = 4$, and 5, the percentage of states for which $E^r_L < \mathcal{G}$ are 33.4%, and 46.8%, respectively, while for the rest of the states, $E^r_L = \mathcal{G}$, up to four decimal places.

IV. LOCAL MEASUREMENT OVER MORE THAN ONE QUBIT CAN BE BETTER

The results on LGGM in the preceding section are obtained by restricting the measurement to a single party. Hence, the question that naturally arises is whether the value of LGGM can be improved by increasing the number of parties, m, over which local measurements can be performed. It is not clear a priori whether increasing the number of measured parties can help to increase localizable entanglement. In this section, we focus on this issue, and discuss several examples of multipartite entangled states in this context.

To begin with, we point out that in the case of the gGHZ state of N qubits, $E^r_L = E^{\mathbf{r}_\alpha}_L$, where $\mathbf{r}_\alpha = \{r_j\}$, $j = 1, 2, \cdots, m$, and $1 < m \le N-2$. This implies that LGGM does not depend on the number of measured qubits for the gGHZ state. The situation, however, can be drastically different if one considers the gW state of N qubits. To demonstrate this, we consider the four-qubit gW state $|W_4\rangle_g = a_1|1000\rangle + a_2|0100\rangle + a_3|0010\rangle + a_4|0001\rangle$, $\{a_i\}$, $i = 1, \cdots, 4$, being real. When $a_1 = a$ and $a_2 = a_3 = a_4 = \sqrt{(1-a^2)/3}$, one finds that for $a \le 1/4$, $\mathcal{G} < E^1_L = E^{\{1,2\}}_L$, while for $a > 1/4$, $\mathcal{G} = E^1_L = E^{\{1,2\}}_L$, where $E^{\{1,2\}}_L$ is the LGGM obtained via measurement over qubits 1 and 2 (see Fig. 3(a)). However, for $a_1 = a$, $a_2 = \sqrt{(1-a^2)/5}$, $a_3 = \sqrt{3(1-a^2)/10}$, and $a_4 = \sqrt{(1-a^2)/2}$, $\mathcal{G} < E^1_L < E^{\{1,2\}}_L$ with $a \le 0.17$, while $\mathcal{G} = E^1_L < E^{\{1,2\}}_L$ when $a > 0.17$. See Fig. 3(b) for a depiction. This is an example for which increasing number of measured qubits enhances the value of LGGM.

The next example is the four-qubit state given by

$$|\Psi_4\rangle = a\Big(|0000\rangle + |0011\rangle + |1100\rangle + |1111\rangle\Big) + \sqrt{\frac{1-a^2}{6}}\Big(|0101\rangle + |1010\rangle + |0110\rangle + |1001\rangle + |1011\rangle + |0100\rangle\Big), \tag{23}$$

where $a \le 1/2$, a being a real number. Similar to the previous example, here also, $E^{\{1,2\}}_L > E^1_L$ for a finite range of the

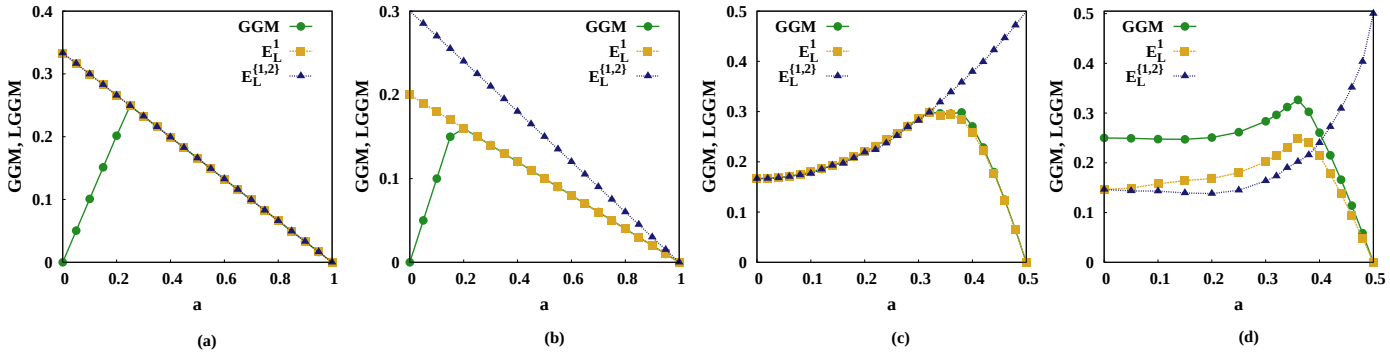

FIG. 3. (Color online.) **(a),(b)** Plot of $\mathcal{G}$, E_L^1, and $E_L^{\{1,2\}}$ as functions of a in case of the four-qubit gW state $|W^4\rangle_g$ with (a) $a_1 = a$, $a_2 = a_3 = a_4 = \sqrt{(1-a^2)/3}$, and (b) $a_1 = a$, $a_2 = \sqrt{(1-a^2)/5}$, $a_3 = \sqrt{3(1-a^2)/10}$, $a_4 = \sqrt{(1-a^2)/2}$. **(c),(d)** Plot of $\mathcal{G}$, E_L^1, and $E_L^{\{1,2\}}$ as functions of a in the case of (c) the four-qubit state $|\Psi_4\rangle$, and (d) the five-qubit state $|\Psi_5\rangle$. All quantities plotted are dimensionless.

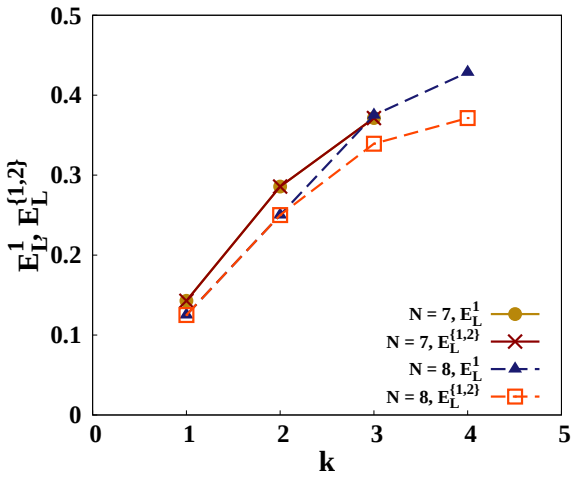

FIG. 4. (Color online.) Plot of $\mathcal{G}$, E_L^1, and $E_L^{\{1,2\}}$ with k for $N = 7$ and $N = 8$ in the case of Dicke states. All quantities plotted are dimensionless.

allowed values of the state-parameter a. However, one must note here that unlike the previous case, there exists parameter ranges in which $E_L^{\{1,2\}} > \mathcal{G} > E_L^1$. It highlights the importance of two-qubit measurement in the cases where single-qubit measurement is not enough to increase the multipartite entanglement possessed by the original state. The variations of $\mathcal{G}$, E_L^1, and $E_L^{\{1,2\}}$, in the case of the four-qubit state $|\Psi_4\rangle$, against the state parameter, a, are shown in Fig. 3(c). Similar examples can also be found in systems constituting of higher number of qubits, as demonstrated for the five-qubit state given by

$$|\Psi_5\rangle = a\Big(|00000\rangle + |00111\rangle + |11000\rangle + |11111\rangle\Big) + \sqrt{\frac{1-a^2}{4}}\Big(|01010\rangle + |10101\rangle + |00001\rangle + |10000\rangle\Big). \quad (24)$$

Here again a finite parameter range can be obtained in which $E_L^{\{1,2\}} > \mathcal{G}$, although $E_L^1 < \mathcal{G}$, as shown in Fig. 3(d). The results of our investigation on the existence arbitrary multiqubit pure states, in which two-qubit measurements may yield better results than single-qubit ones, are presented in Sec. V. Intuitively, one can argue that if one increases the number of parties in which the measurement is performed, it helps to concentrate entanglement and hence to increase LGGM. The above examples support such intuition. However, let us present here the case of N-qubit Dicke states for which such intuition fails. In particular, we find that $E_L^{\{1,2\}}$ is not beneficial compared to E_L^1 in the case of a Dicke state. We determine the values of E_L^1 and $E_L^{\{1,2\}}$ in the case of $|D_k^N\rangle$ with $4 \leq N \leq 10$, for different allowed values of k. We find that irrespective of the value of N and k, $E_L^{\{1,2\}} \leq E_L^1 \leq \mathcal{G}$ for Dicke states. The variations of $\mathcal{G}$, E_L^1, and $E_L^{\{1,2\}}$ against different values of k for $N = 7$ and 8 are shown in Fig. 4, while the variations of E_L^1 and $E_L^{\{1,2\}}$ with varying k, for $N = 9$ and 10, are qualitatively similar to that for $N = 7$ and 8 respectively. The question of whether this is a generic property of the symmetric states is discussed in the next section.

V. ARBITRARY N-QUBIT PURE STATES: NUMERICAL RESULTS

In this section, we present the numerical results regarding arbitrary N-qubit pure states, and compare advantages of multiqubit measurements over single-qubit ones.

A. Arbitrary tripartite pure states

We investigate here the behavior of LGGM in the case of arbitrary pure states of three-qubits. We separately consider three-qubit states belonging to the paradigmatic GHZ and the W classes [32, 35, 37, 38], which belong to mutually disjoint sets that together construct the entire set of three-qubit pure states. The normalized three-qubit states of the W-class are given by [38]

$$|\Phi_w\rangle = \sqrt{a_1}|001\rangle + \sqrt{a_2}|010\rangle + \sqrt{a_3}|100\rangle + \sqrt{a_4}|000\rangle \quad (25)$$

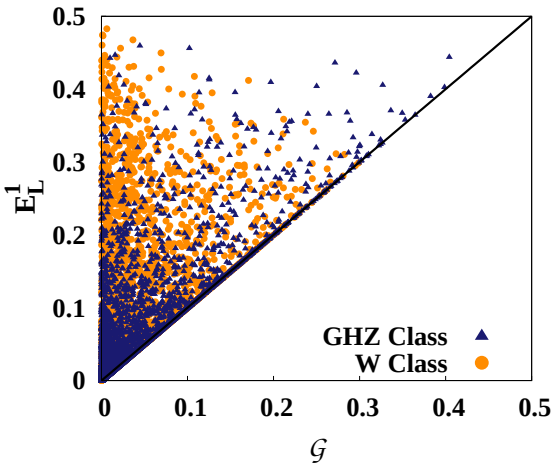

FIG. 5. (Color online.) Plot of E_L^1 vs. $\mathcal{G}$ for 10^5 Haar-uniformly generated three-qubit pure states belonging to (a) the GHZ class, and (b) the W class. For both the classes, $E_L^1 \geq \mathcal{G}$. All quantities plotted are dimensionless.

with $a_1, a_2, a_3 > 0$, and $a_4 = 1 - (a_1 + a_2 + a_3) \geq 0$. Simple algebra dictates that the GGM of $|\Phi_w\rangle$ is given by $\mathcal{G} = 1 - \max\{\lambda_i\}$, $i = 1, 2, 3$, where $\lambda_i = [1+(1-4((a_j+a_k)a_i)^{1/2}]/2$, with $i, j, k \in \{1, 2, 3\}$, and no two among i, j, k being equal. Now, LGGM of $|\Phi_w\rangle$ for $r = 1$ can be obtained as $E_L^1 = [1 - \min_{\theta,\phi} f_{wc}(\theta, \phi)]/2$, where

$$f_{wc}(\theta, \phi) = \sum_{l=1}^{2} (p^{l\,2} - 4a_1 a_2 u^l)^{1/2}, \tag{26}$$

and $p^l = (a_1 + a_2 + a_4)q_1^l + a_3 q_2^l - (-1)^l \sqrt{a_3 a_4} s_\theta c_\phi$, with $q_{1,2}^l$ and u^l given in Eqs. (10) and (15), respectively. The optimization of the above function leads to two equations involving the real parameters θ and ϕ. One of them implies $\phi = 0, \pi$ independent of the value of θ, while the second equation, independent of ϕ, has to be solved numerically for θ. Numerical solution of the latter provides the values of θ, which, along with $\phi = 0, \pi$, makes the Jacobian of $f_{wc}(\theta, \phi)$ positive semidefinite.

The normalized three-qubit states of the GHZ class can be represented by [38]

$$|\Phi_{ghz}\rangle = \sqrt{K} \left(c_\delta |000\rangle + e^{i\mu} s_\delta \bigotimes_{i=1}^{3} |\eta_i\rangle \right),$$

where $|\eta_i\rangle = c_{\gamma_i}|0\rangle + s_{\gamma_i}|1\rangle$, and $K^{-1} = 1 + 2c_\delta s_\delta c_{\gamma_1} c_{\gamma_2} c_{\gamma_3} c_\mu$, K being the normalization factor, and $K \in (1/2, \infty)$. The ranges for the five real parameters are $\delta \in (0, \pi/4]$, $\gamma_i \in (0, \pi/2]$, $i = 1, 2, 3$, and $\mu \in [0, 2\pi)$. To determine and compare the behavior of LGGM to that of GGM of the states belonging to the GHZ and W class, we Haar-uniformly generate 10^5 three-qubit pure states belonging to each of the classes, and calculate E_L^1 and $\mathcal{G}$. The scatter-plot of E_L^1 versus $\mathcal{G}$ is shown in Fig. 5. For all the randomly generated three-qubit pure states belonging to both the GHZ and the W classes, we find that $E_L^1 \geq \mathcal{G}$ (see Fig. 5), the equality is considered when $E_L^r = \mathcal{G}$ up to four decimal places.

Motivated by the findings in the case of three-qubit gW state, we investigate whether the maximal Schmidt coefficient being found across a certain r':rest bipartition in the case of an arbitrary three-qubit pure state, i.e., the GGM is a function of the maximal Schmidt coefficient in the r':rest split, ensures that the global LGGM, $E_{GL} = E_L^{r'}$, where r' can be 1, 2, or 3. To test this, we perform an extensive numerical search over a set of 10^7 three-qubit pure states from each of the W and the GHZ classes. We find that for all instances, $E_{GL} = E_L^{r'}$, when the bipartition r':rest provides $\mathcal{G}$. In the case of the W class as well as the GHZ class of states, $E_L^r = \mathcal{G}$, up to four decimal places when $r \neq r'$. These observations lead to the following conjectures:

If the maximal Schmidt coefficient for an arbitrary three-qubit pure state is obtained across the bipartition r:rest, $r \in \{1, 2, 3\}$, then $E_{GL} = E_L^{r'} \geq \mathcal{G}$ with $r' \in \{1, 2, 3\}$ when $r' = r$. On the other hand, $E_L^{r'}$ coincides with $\mathcal{G}$ when $r' \neq r$.

These conjectures help to pin-point the position of measurement while one tries to increase the value of genuine multiparty entanglement by means of localization.

B. N-qubit states: Single-qubit measurement vs. local measurements over more than one qubit

To visualize the behavior of LGGM and its relation with the GGM for arbitrary N-qubit states, we now Haar uniformly generate four- and five-qubit pure states and study the variation of LGGM with respect to the GGM of the original states.

Single-qubit measurement

First, we focus on the case of measurement over a single qubit. Fig. 6(a) depicts the variation of the LGGM of 10^5 Haar uniformly chosen random states for each of the forms $|\Psi_i^4\rangle$, $i = 1, 2, \cdots, 6$, from the nine classes of four-qubit states [48, 49], against their GGM, when local rank-1 projective measurement is performed over qubit 1. A short description of the parametrized forms of the nine classes of four-qubit states is given in the Appendix. Note that in all instances except $|\Psi_6^4\rangle$, the LGGM is found to be upper bounded by the GGM of the original state. This result remains unchanged with a change in the position of the measured qubit, as indicated by Fig. 6(b), where results corresponding to measurement over qubit 2 in the cases of $|\Psi_3^4\rangle$, $|\Psi_5^4\rangle$, and $|\Psi_6^4\rangle$ are presented.

The LGGM of the states $|\Psi_i^4\rangle$, $i = 7, 8, 9$, can be obtained analytically, and are tabulated in Table II. when a measurement over qubit r, $r = 1, 2, 3, 4$, is performed. The corresponding GGM is also tabulated. Note here that the state $|\Psi_9^4\rangle$ can be written as the product of $|0\rangle_1$ in the first qubit, and a GHZ state in the remaining three qubits. Therefore, upon measurement over the qubit 1, it provides an example of $\mathcal{G} = 0$ with $E_L^1 = 1/2$, which is similar to the case of a product of $|0\rangle$ and singlet. Note also that $|\Psi_8^4\rangle$ presents an example of a four-qubit state for which a higher value of LGGM than that of the GGM is found only when measurement is performed over a specific qubit, while in the case of $|\Psi_7^4\rangle$, single-qubit measurement can not increase the value of LGGM than that of GGM.

State	$\mathcal{G}$	$\mathbf{E_L^1}$	$\mathbf{E_L^2}$	$\mathbf{E_L^3}$	$\mathbf{E_L^4}$	$\mathbf{E_L^{\{1,2\}}}$	$\mathbf{E_L^{\{1,3\}}}$	$\mathbf{E_L^{\{1,4\}}}$	$\mathbf{E_L^{\{2,3\}}}$	$\mathbf{E_L^{\{2,4\}}}$	$\mathbf{E_L^{\{3,4\}}}$
$\|\Psi_7^4\rangle$	1/4	1/4	1/4	1/4	1/4	1/4	1/4	1/4	1/4	1/4	1/4
$\|\Psi_8^4\rangle$	1/4	1/2	1/4	1/4	1/4	1/2	1/2	1/2	1/2	1/2	1/4
$\|\Psi_9^4\rangle$	0	1/2	0	0	0	1/2	1/2	1/2	1/2	1/2	0

TABLE II. The values of $\mathcal{G}$, E_L^r ($r = 1, 2, 3, 4$), and $E_L^{\{r_1,r_2\}}$ ($r_1 \neq r_2$, $r_{1,2} \in \{1, 2, 3, 4\}$) for the four-qubit states $|\Psi_7^4\rangle$, $|\Psi_8^4\rangle$, and $|\Psi_9^4\rangle$.

Local measurements over two qubits

The question that naturally arises is whether the value of LGGM of a particular N-qubit state can be increased by performing measurements over more than one qubit. To investigate this, we consider local measurements over two-qubits, and study the behavior of LGGM in the case of randomly sampled four- and five-qubit states. Contrary to the result obtained above for the classes of four-qubit states, in the case of Haar-uniformly generated arbitrary four-qubit pure states, about 29% of states are found to have $E_L^1 > \mathcal{G}$, as depicted for a set of 10^5 states in Fig. 7(a). Interestingly, when local measurements over qubits 1 and 2 are performed, about 22% of the 71% states for which $\mathcal{G} > E_L^1$ are found to have $E_L^{\{1,2\}} > \mathcal{G}$. Also, for about 47.6% of such states, $E_L^{\{1,2\}} > E_L^1$. Qualitatively similar results are found when random four-qubit states are sampled Haar-uniformly from the parametrized four-qubit classes [48, 49]. For example, the LGGM of about 20.4% of the four-qubit states of the form $|\Psi_1^4\rangle$, for which $E_L^1 \leq \mathcal{G}$, can be increased beyond the value of $\mathcal{G}$, when local measurements over qubits 1 and 2 are performed (Fig. 7(b)). Moreover, for about 44.9% of the states, $E_L^{\{1,2\}} > E_L^1$. The values of $E_L^{\{r_1,r_2\}}$, where $r_1 \neq r_2$ with $r_{1,2} \in \{1, 2, 3, 4\}$, in the case of the states $|\Psi_i^4\rangle$, $i = 7, 8, 9$, are tabulated in Table II. Note that the state $|\Psi_7^4\rangle$, provides an example of a four-qubit pure state for which $E_L^{\mathbf{r}_\alpha} = \mathcal{G}\ \forall\ \mathbf{r}_\alpha$, where $\alpha = 1, 2, \cdots, \binom{N}{m}$, $m = 1, 2$.

Next, we consider the symmetric states in the form of generalized superposition of Dicke states. To test the effect of an increase in the number of measured qubits on the value of LGGM of $|D_g^N\rangle$, we consider a set of 10^5 Haar-uniformly chosen such states from each of the cases of $N = 4$ and $N = 5$. Note here that the symmetry present in the states $|D_g^N\rangle$ guarantees that all pairs of qubits chosen for local measurement are equivalent. Similar to the case of single-qubit measurement, in the case of $m = 2$ also, $E_L^{\{r_1,r_2\}} \leq \mathcal{G}$, where $r_1 \neq r_2$, and $r_{1,2} \in \{1, 2, \cdots, N\}$. However, in contrast to the previous examples of two-qubit measurements, in this case, an increase in m is found to result, for an overwhelmingly large fraction of states, in a decrease in the value of LGGM. For example, in about 99.1% of $|D_g^4\rangle$, $E_L^{\{r_1,r_2\}} < E_L^1$, while for $N = 5$, the fraction is 93.9%. The variation of LGGM against GGM for the four-qubit states of the form $|D_g^4\rangle$ is depicted in Fig. 7(c). See Fig. 7(d) for results on arbitrary five-qubit pure states.

VI. LGGM IN QUANTUM SPIN MODELS

For the past fifteen years or so, probing interesting physical phenomena observed in many-body systems using quantum information theoretic tools and techniques has been an active cross-disciplinary field of research [12–14, 50–52]. Realization of quantum spin Hamiltonians in various substrates, such as solid state systems [53], optical lattice [20, 54, 55], ion traps [12, 56], and NMR [57] under controlled laboratory environments have allowed researchers to test the properties of several information theoretic measures of quantum correlations in well-known quantum spin models. In this section, we discuss the behavior of LGGM in the vicinity of quantum phase transitions [42], when the pure state, for which LGGM is calculated, is the ground state of well-known one-dimensional (1d) quantum spin models.

It is interesting to mention here that a similar set of results were obtained in Ref. [36] by using the concept of localizable entanglement. An important difference of the results there with those in this paper is that the plots and the corresponding analyses here are directly for the LGGM, while those in Ref. [36] are often for bounds on localizable entanglement.

A. Transverse-field Ising Model

The first model we discuss is the transverse-field quantum Ising model [43] with periodic boundary condition (PBC), whose Hamiltonian is given by

$$H = J \sum_{i=1}^{N} \sigma_i^x \sigma_{i+1}^x + h \sum_{i=1}^{N} \sigma_i^z. \tag{27}$$

Here, J and h are strengths of respectively the nearest-neighbor coupling and the external magnetic field, $\sigma_i^{x,z}$ are the Pauli spin matrices, and N is the number of qubits in the system. Under PBC, $\sigma_{N+1} \equiv \sigma_1$. Both J and h are > 0.

The 1d transverse-field Ising model is known to undergo a quantum phase transition at the critical value of the parameter $\lambda = \lambda_c \equiv 1$ [13, 14, 42, 43, 50, 51], where $\lambda = J/h$, from an anti-ferromagnetic ($J > h$) to a paramagnetic phase ($J < h$). Although a few studies of the behavior of multipartite entanglement measures across QPT in quantum spin models are available [9, 10, 52], the investigation is restricted mainly due to the difficulty of computing multiparty entanglement measures.

The transverse Ising model can be solved by using the Jordan-Wigner transformation, followed by Fourier and Bogoliubov transformations [43]. However, this does not result in an analytical form for the LGGM. Therefore, we numerically investigate the behavior of LGGM in the case of the transverse-field Ising model, and determine the ground state of the model for $N = 6$, 8, and 10 spins via exact diagonalization. By performing numerical optimization, $\mathcal{G}$, E_L^1, and $E_L^{\{1,2\}}$ are determined as functions of λ. Fig. 8(a) depicts the variation of GGM as well as LGGM with respect to λ for $N = 8$, while the inset shows

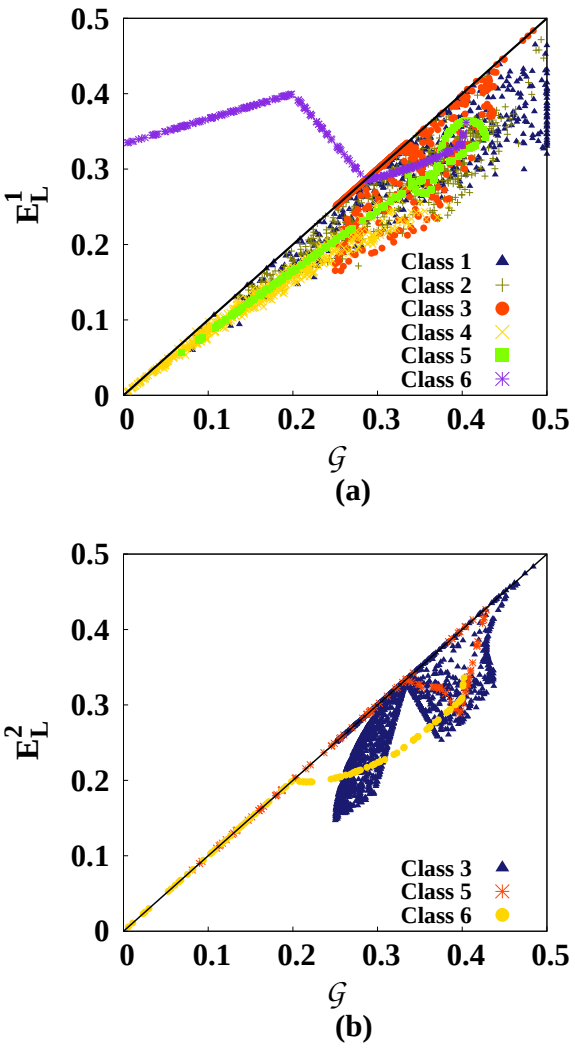

FIG. 6. (Color online.) **(a)** Scatter plot of E_L^1 vs. $\mathcal{G}$ for the four-qubit classes represented by $|\Psi_i^4\rangle$, $i = 1, \cdots, 6$. For all the classes except $i = 6$, $E_L^1 \leq \mathcal{G}$. The scatter plot is obtained by Haar-uniformly generating 10^5 random four-qubit states from each of the six classes. **(b)** Scatter plot for E_L^2 vs. $\mathcal{G}$ for the four-qubit classes represented by $|\Psi_i^4\rangle$, $i = 3, 5, 6$. Unlike the case described in Fig. 6(a), here, for all the classes, $E_L^2 \leq \mathcal{G}$, where the equality is considered when $E_L^2 = \mathcal{G}$ up to four decimal points. The scatter plot is obtained by Haar-uniformly generating 10^5 random four-qubit states from each of the three classes. All quantities plotted are dimensionless.

the behavior of the first derivatives of GGM and LGGM w.r.t. λ, which exhibit peaks at $\lambda = 0.969$, 0.996 and 0.996 for $\mathcal{G}$, E_L^1, and $E_L^{\{1,2\}}$, respectively. Note that the position of the QPT point signaled by the multiparty measures are close to the QPT point $\lambda = \lambda_c \equiv 1$. Note also that the result is better in the case of LGGM when compared to that obtained for GGM. In order to investigate how the result changes if the system size increases, we perform the same analysis for the transverse-field Ising model defined on $N = 6$ and $N = 10$ qubits. Fig. 8(b) and (c) presents the behavior of the first derivative of $\mathcal{G}$, E_L^1, and $E_L^{\{1,2\}}$ w.r.t. λ for $N = 6$ and $N = 10$, respectively. For $N = 6$, the position of the QPT, as signaled by $\mathcal{G}$, E_L^1, and $E_L^{\{1,2\}}$ are $\lambda = 0.950, 0.988$, and 1.011 respectively. On the other hand, for $N = 10$, the signature of QPT is obtained at $\lambda = 0.979$, 1.0002, and 1.003 for $\mathcal{G}$, E_L^1, and $E_L^{\{1,2\}}$ respectively, which clearly indicates an improvement with an increase in the system size.

B. XXZ model in an external field

The Hamiltonian describing the 1d XXZ model [44–47], under PBC, is given by

$$H' = -J' \sum_{i=1}^{N} (\sigma_i^x \sigma_{i+1}^x + \sigma_i^y \sigma_{i+1}^y + \Delta \sigma_i^z \sigma_{i+1}^z) - h' \sum_{i=1}^{N} \sigma_i^z), \tag{28}$$

where J' and h' represent respectively the nearest-neighbor coupling and the external field-strength, while Δ is the (dimensionless) anisotropy in the z direction. The model can be solved using the Bethe ansatz [44], but an analytical form of the LGGM is difficult to obtain. We probe the rich phase diagram [47] of this model using LGGM as the observable, where the ground state is obtained via exact diagonalization for different values of the system parameters, Δ and h'/J'.

Fig. 9(a) shows the variations of $\mathcal{G}$, E_L^1, and $E_L^{\{1,2\}}$ against h'/J' for the ground state of the Hamiltonian given in Eq. (28) with $N = 8$ with $\Delta = 0.5$. All the multipartite observables goes sharply to zero at $h'/J' = 1$, signaling a crossing of the ground state and the first excited state energy levels [45, 47]. The inset of Fig. 9(a) shows the variation of $\mathcal{G}$, E_L^1, and $E_L^{\{1,2\}}$ with h'/J' for $\Delta = -2$, in which case the system undergoes a QPT from the gapless to the gapped phase at $h'/J' = 6$, indicated by a sudden drop in values of GGM as well as LGGM to zero.

In the absence of the external magnetic field, the ground state of the model experiences a KT transition [45] at $\Delta = -1$, which is signaled by a blunt minimum in the $\mathcal{G}$ vs. Δ curve (see Fig. 9(b)). On the other hand, the LGGMs, namely E_L^1 and $E_L^{\{1,2\}}$, show a sharp cusp at $\Delta = -1$, correctly signaling the KT transition. Note here that the changes in the value of $\mathcal{G}$ with Δ occurs in the third decimal place, while the variation in LGGM takes place in the second decimal point, indicating a sharper detector of the QPT in comparison with that shown by GGM. Note also that similar to localizable entanglement [36], LGGM also signals the KT transition, which is usually not detected by the frequently-used quantum information theoretic observables in detecting QPTs [58].

Note here that even for a small system where finite-size effects are expected to play a considerable role, LGGM serves as a satisfactory indicator of quantum critical phenomena, and in all these examples, shows that it can act as a more powerful detector than the other multipartite entanglement measures. Hence, LGGM is expected to find its applicability in the investigation of quantum cooperative phenomena observed in many-body systems beyond the quantum spin chain models.

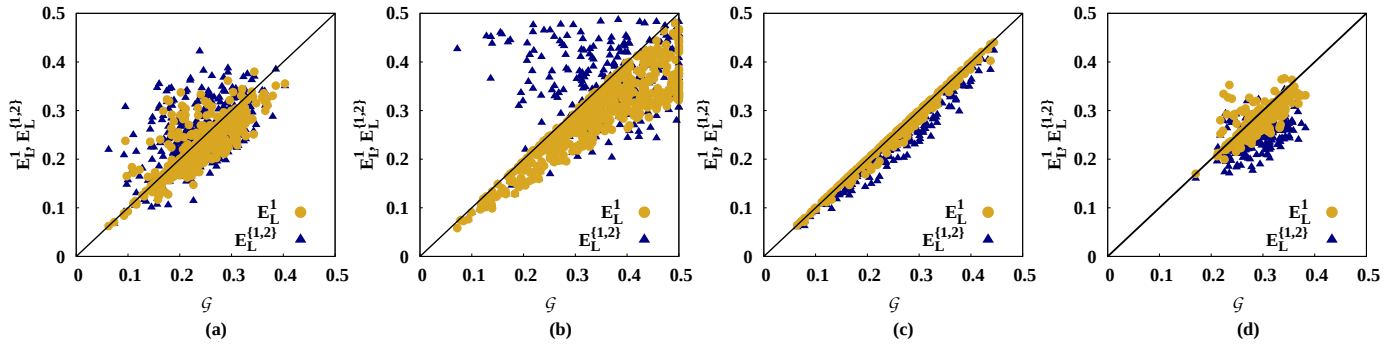

FIG. 7. Scatter plot for E_L^1 vs. $\mathcal{G}$ and $E_L^{\{1,2\}}$ vs. $\mathcal{G}$ in the case of (a) arbitrary four-qubit pure states, (b) four-qubit states of the form $|\Psi_1^4\rangle$, (c) four-qubit symmetric states of the form $|D_g^N\rangle$, and (d) arbitrary five-qubit pure states. For each of the cases, the scatter diagram is obtained by Haar-uniformly generating a set of 10^5 random states of the respective types. All quantities plotted are dimensionless.

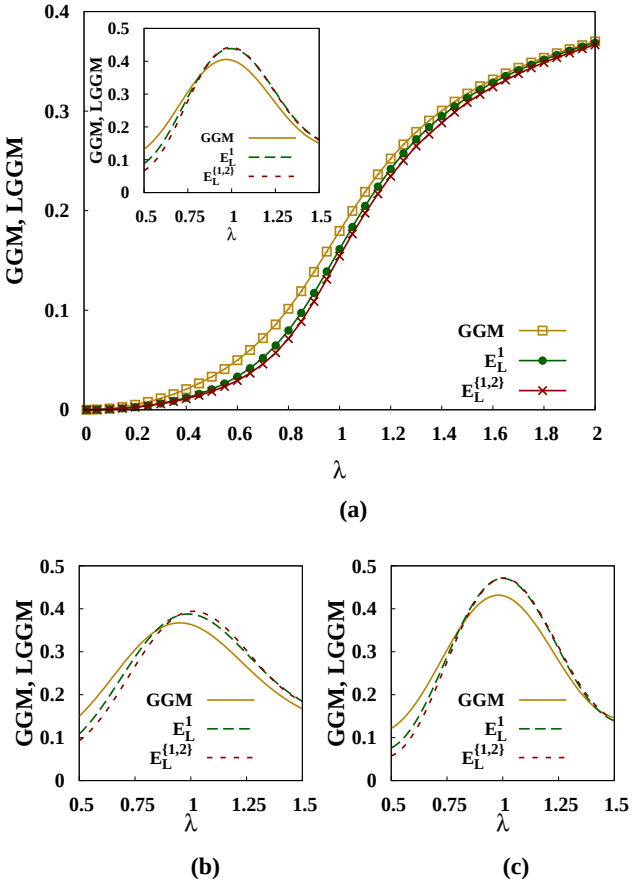

FIG. 8. (Color online.) **(a)** Variations of $\mathcal{G}$, E_L^1, and $E_L^{\{1,2\}}$ as functions of $\lambda = J/h$ for the transverse-field Ising model with $N = 8$. The first derivatives of $\mathcal{G}$, E_L^1, and $E_L^{\{1,2\}}$ show peaks at $\lambda = 0.969$, 0.996, and 0.996, respectively, as shown in the inset. **(b)** Variations of the first derivatives of $\mathcal{G}$, E_L^1, and $E_L^{\{1,2\}}$ for $N = 6$. The peaks now occur at $\lambda = 0.950$, 0.988, and 1.011 in the cases of $\mathcal{G}$, E_L^1, and $E_L^{\{1,2\}}$ respectively. **(c)** Variations of the first derivatives of $\mathcal{G}$, E_L^1, and $E_L^{\{1,2\}}$ as functions of λ for the transverse-field Ising model with $N = 10$. The peaks now occur at $\lambda = 0.979$, 1.0002, and 1.003 in the case of $\mathcal{G}$, E_L^1, and $E_L^{\{1,2\}}$ respectively. All quantities plotted are dimensionless.

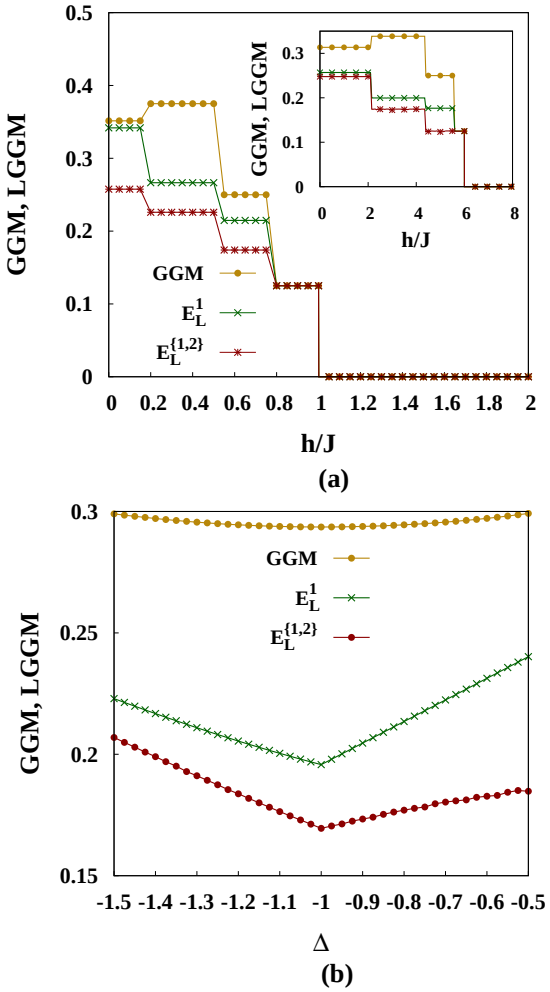

FIG. 9. (Color online.) **(a)** Variations of $\mathcal{G}$, E_L^1, and $E_L^{\{1,2\}}$ as functions of h'/J' for $\Delta = 0.5$ and (inset) $\Delta = -2$. **(b)** Variations of $\mathcal{G}$, E_L^1, and $E_L^{\{1,2\}}$ as functions of Δ at $h = 0$. All quantities plotted are dimensionless.

VII. CONCLUDING REMARKS

Multipartite entanglement has been proven to be useful for the successful implementation of several quantum information theoretic protocols. In the present paper, we consider the conceptualization and use of localizable multipartite entanglement, obtained by performing a local measurement at a few parties. The notion of localizable multiparty entanglement depends on the understanding and computability of another measure of multiparty entanglement of a lower number of parties, which we refer to as the seed measure. We use the geometric measure in general, and the generalized geometric measure in particular, as the see measure. In the case when the seed measure is the generalized geometric measure, the localizable multiparty entanglement measure is called the localizable generalized geometric measure. We discuss its various properties, and in particular, we analytically consider the behavior of the measure for a number of paradigmatic examples of multipartite pure states, where the localization is achieved via local rank-1 projective measurement over a single qubit. The examples include the N-qubit generalized GHZ and W states, Dicke states, and the generalized superposition of Dicke states for fixed number of qubits. We show that for the N-qubit generalized GHZ and W states, the localization of generalized geometric measure by local projection measurement over one qubit always results in a value of localizable multipartite entanglement which is greater than, or equal to the multipartite entanglement present in the original state. Our numerical simulations seem to indicate that such enhancement due to measurement holds for arbitrary three-qubit pure states. However, for higher number of parties, no such lower bound exists. We also show that for the N-qubit Dicke states, the localizable multipartite entanglement achieved via single-qubit measurement is bounded above by the generalized geometric measure of the original state.

To investigate whether measurement over more than one qubit helps in achieving a better localization of multipartite entanglement than a single-qubit measurement, we consider several examples of multi-qubit pure states. We show that there exists multiqubit states in which local measurement over two qubits yields higher values of localizable generalized geometric measure compared to single-qubit measurement. However, this phenomenon is not generic for arbitrary multiqubit states, as shown from our numerical simulations. We finally inquire whether there exists a situation in which LGGM is more powerful than its parent multipartite entanglement measure, the GGM. We show that this is indeed the case for detecting QPT in the many-body systems. Specifically, we show that the derivatives of LGGM can signal QPT of the transverse-field Ising model more accurately even for a smaller system-size, achievable in current experiments, compared to that of the GGM. We also show that LGGM detects the KT transition of the XXZ model better than its parent multiparty measure.

APPENDIX

Classes of four-qubit states

The nine classes of four-qubit states, as considered in [48, 49], are

$$
\begin{aligned}
|\Psi_1^4\rangle &= \frac{a_1+a_2}{2}(|0000\rangle+|1111\rangle)+\frac{a_1-a_2}{2}(|0011\rangle+|1100\rangle)+\frac{a_3+a_4}{2}(|0101\rangle+|1010\rangle)+\frac{a_3-a_4}{2}(|0110\rangle+|1001\rangle),\\
|\Psi_2^4\rangle &= \frac{a_1+a_2}{2}(|0000\rangle+|1111\rangle)+\frac{a_1-a_2}{2}(|0011\rangle+|1100\rangle)+a_3(|0101\rangle+|1010\rangle+|0110\rangle),\\
|\Psi_3^4\rangle &= a_1(|0000\rangle+|1111\rangle)+a_2(|0101\rangle+|1010\rangle+|0110\rangle+|0011\rangle),\\
|\Psi_4^4\rangle &= a_1(|0000\rangle+|1111\rangle)+\frac{a_1+a_2}{2}(|0101\rangle+|1010\rangle)+\frac{a_1-a_2}{2}(|0110\rangle+|1001\rangle)+\frac{i}{\sqrt{2}}(|0001\rangle+|0010\rangle+|0111\rangle+|1011\rangle),\\
|\Psi_5^4\rangle &= a_1(|0000\rangle+|0101\rangle+|1010\rangle+|1111\rangle)+i|0001\rangle+|0110\rangle-i|1011\rangle,\\
|\Psi_6^4\rangle &= a_1(|0000\rangle+|1111\rangle)+|0011\rangle+|0101\rangle+|0110\rangle,\\
|\Psi_7^4\rangle &= |0000\rangle+|0101\rangle+|1000\rangle+|1110\rangle,\\
|\Psi_8^4\rangle &= |0000\rangle+|1011\rangle+|1101\rangle+|1110\rangle,\\
|\Psi_9^4\rangle &= |0000\rangle+|0111\rangle,
\end{aligned}
\tag{29}
$$

where the complex parameters a_1, a_2, a_3, and a_4 have non-negative real parts.

[1] R. Horodecki, P. Horodecki, M. Horodecki, and K. Horodecki, Rev. Mod. Phys. **81**, 2 (2009).

[2] R. Raussendorf and H. J. Briegel, Phys. Rev. Lett. **86**, 5188 (2001); P. Walther, K. J. Resch, T. Rudolph, E. Schenck, H. Weinfurter, V. Vedral, M. Aspelmeyer, and A. Zeilinger, Nature **434**, 169 (2005); H. J. Briegel, D. Browne, W. Dür, R. Raussendorf, and M. van den Nest, Nat. Phys. **5**, 19 (2009).

[3] C. H. Bennet and S. J. Wiesner, Phys. Rev. Lett. **69**, 2881 (1992); K. Mattle, H. Weinfurter, P. G. Kwiat, and A. Zeilinger, Phys. Rev. Lett. **76**, 4656 (1996).

[4] D. Bruß, G. M. D'Ariano, M. Lewenstein, C. Macchiavello, A. Sen(De), and U. Sen, Phys. Rev. Lett. 93, 210501 (2004); D. Bruß,

G. M. D'Ariano, M. Lewenstein, C. Macchiavello, A. Sen(De), and U. Sen, Int. J. Quant. Inf. **4**, 415-428 (2006).

[5] See A. Sen(De) and U. Sen, Physics News **40**, 17-32 (2010) (arXiv:1105.2412 [quant-ph]) for a review on quantum communication protocols.

[6] A. Ekert, Phys. Rev. Lett. **67**, 661 (1991); T. Jennewein, C. Simon, G. Weihs, H. Weinfurter, and A. Zeilinger, Phys. Rev. Lett. **84**, 4729 (2000); D. S. Naik, C. G. Peterson, A. G. White, A. J. Berglund, and P. G. Kwiat, Phys. Rev. Lett. **84**, 4733 (2000); W. Tittel, T. Brendel, H. Zbinden, and N. Gisin, Phys. Rev. Lett. **84**, 4737 (2000); N. Gisin, G. Ribordy, W. Tittel, and H. Zbinden, Rev. Mod. Phys. **74**, 145 (2002).

[7] M. Żukowski, A. Zeilinger, M. A. Horne, and H. Weinfurter, Acta Phys. Pol. **93**, 187 (1998); M. Hillery, Vladimír Bužek, and André Berthiaume, Phys. Rev. A **59**, 1829 (1999); R. Demkowicz-Dobrzanski, A. Sen(De), U. Sen, and M. Lewenstein, Phys. Rev. A **80**, 012311 (2009).

[8] R. Cleve, D. Gottesman, and H.-K. Lo, Phys. Rev. Lett. **83**, 648 (1999); A. Karlsson, M. Koashi, and N. Imoto, Phys. Rev. A **59**, 162 (1999).

[9] T.-C. Wei, D. Das, S. Mukhopadyay, S. Vishveshwara, and P. M. Goldbart, Phys. Rev. A **71**, 060305(R) (2005); R. Orús, Phys. Rev. Lett. **100**, 130502 (2008); R. Orús, S. Dusuel, and J. Vidal, ibid. **101**, 025701 (2008); R. Orús, Phys. Rev. A **78**, 062332 (2008); Q.-Q. Shi, R. Orús, J. O. Fjærestad, and H.-Q. Zhou, New J. Phys. **12**, 025008 (2010). R. Orús and T.-C. Wei, Phys. Rev. B **82**, 155120 (2010); A. Sen(De) and U. Sen, arXiv:1002.1253 (2010); R. Prabhu, S. Pradhan, A. Sen(De), and U. Sen, Phys. Rev. A **84**, 042334 (2011); H. S. Dhar and A. Sen(De), J. Phys. A: Math. Theor. **44**, 465302 (2011); H. S. Dhar, A. Sen(De), and U. Sen, New J. Phys. **15**, 013043 (2013).

[10] A. Biswas, R. Prabhu, A. Sen(De), and U. Sen, Phys. Rev. A **90**, 032301 (2014).

[11] M. Sarovar, A. Ishizaki, G. R. Fleming, and K. B. Whaley, Nat. Phys. **6**, 462 (2010); J. Zhu, S. Kais, A. Aspuru-Guzik, S. Rodriques, B. Brock, and P. J. Love, J. Chem. Phys. **137**, 074112 (2012); N. Lambert, Y.-N. Chen, Y.-C. Cheng, C.-M. Li, G.-Y. Chen, and F. Nori, Nat. Phys. **9**, 10 (2013); T. Chanda, U. Mishra, A. Sen(De), and U. Sen, arXiv:1412.6519v2 [quant-ph] (2014), and references therein.

[12] M. Lewenstein, A. Sanpera, V. Ahufinger, B. Damski, A. Sen(De), and U. Sen, Adv. Phys. **56**, 243 (2007).

[13] L. Amico, R. Fazio, A. Osterloh, and V. Vedral, Rev. Mod. Phys. **80**, 517 (2008).

[14] K. Modi, A. Brodutch, H. Cable, T. Paterek, and V. Vedral, Rev. Mod. Phys. **84**, 1655 (2012).

[15] M.-F. Yang, Phys. Rev. A **71**, 030302 (2005); X.-F. Qian, T. Shi, Y. Li, Z. Song, and C.-P. Sun, Phys. Rev. A **72**, 012333 (2005); P. Lou and J.Y. Lee, Phys. Rev. B **74**, 134402 (2006); R. W. Chhajlany, P. Tomczak, A. Wójcik, and J. Richter, Phys. Rev. A **75**, 032340 (2007); D.I. Tsomokos, J.J. Garc a-Ripoll, N.R. Cooper, and J.K. Pachos, Phys. Rev. A **77**, 012106 (2008); C.-S. Yu, L. Zhou, and H.-S. Song, ibid. **77**, 022313 (2008); Z. Sun, X.-M. Lu, H.-N. Xiong, and J. Ma, New J. Phys. **11**, 113005 (2009); X. Peng, J. Zhang, J. Du, and D. Suter, Phys. Rev. A **81**, 042327 (2010); M. N. Bera, R. Prabhu, A. Sen(De), and U. Sen, arXiv:1209.1523 [quant-ph] (2012).

[16] D. Leibfried, E. Knill, S. Seidelin, J. Britton, R. B. Blakestad, J. Chiaverini, D. B. Hume, W. M. Itano1, J. D. Jost, C. Langer, R. Ozeri1, R. Reichle, and D. J. Wineland, Nature **438**, 639 (2005); T. Monz, P. Schindler, J. T. Barreiro, M. Chwalla, D. Nigg, W. A. Coish, M. Harlander, W. Hansel, M. Hennrich, and R. Blatt, Phys. Rev. Lett. **106**, 130506 (2011). J.T. Barreiro, J.-D. Bancal, P. Schindler, D. Nigg, M. Hennrich, T. Monz, N. Gisin and R. Blatt, Nat. Phys. **9**, 559 (2013), and references therein.

[17] R. Prevedel, G. Cronenberg, M. S. Tame, M. Paternostro, P. Walther, M. S. Kim, and A. Zeilinger, Phys. Rev. Lett. **103**, 020503 (2009); W.-B. Gao, C.-Y. Lu, X.-C. Yao, P. Xu, O. Gühne, A. Goebel, Y.-A. Chen, C.-Z. Peng, Z.-B. Chen, and J.-W. Pan, Nat. Phys. **6**, 331 (2010); Y.-F. Huang, B.-H. Liu, L. Peng, Y.-H. Li, L. Li, C.-F. Li, and G.-C. Guo, Nat. Comms. **2**, 546 (2011); X.-C. Yao, T.-X. Wang, P. Xu, H. Lu, G.-S. Pan, X-H. Bao, C.- Z. Peng, C.-Y. Lu, Y.-A. Chen, and J.-W. Pan, Nat. Photonics **6**, 225 (2012), and references therein.

[18] R. Barends, J. Kelly, A. Megrant, A. Veitia, D. Sank, E. Jeffrey, T. C. White, J. Mutus, A. G. Fowler, B. Campbell, Y. Chen, Z. Chen, B. Chiaro, A. Dunsworth, C. Neill, P. OMalley, P. Roushan, A. Vainsencher, J. Wenner, A. N. Korotkov, A. N. Cleland, and J. M. Martinis, Nature **508**, 500 (2014), and references therein.

[19] C. Negrevergne, T.S. Mahesh, C.A. Ryan, M. Ditty, F. Cyr-Racine, W. Power, N. Boulant, T. Havel, D.G. Cory, and R. Laflamme, Phys. Rev. Lett. **96**, 170501 (2006), and references therein.

[20] O. Mandel, M. Greiner, A. Widera, T. Rom, T.W. Hänsch, and I. Bloch, Nature **425**, 937 (2003); I. Bloch, J. Phys. B: At. Mol. Opt. Phys. **38**, S629 (2005); P. Treutlein, T. Steinmetz, Y. Colombe, B. Lev, P. Hommelhoff, J. Reichel, M. Greiner, O. Mandel, A. Widera, T. Rom, I. Bloch, and T. W. Hänsch, Fortschr. Phys. **54**, 702 (2006); M. Cramer, A. Bernard, N. Fabbri, L. Fallani, C. Fort, S. Rosi, F. Caruso, M. Inguscio, and M.B. Plenio, Nat. Comm. **4**, 2161 (2013), and references therein.

[21] J. M. Raimond, M. Brune, and S. Haroche, Rev. Mod. Phys. **73**, 565 (2001); D. Leibfried, R. Blatt, C. Monroe, and D. Wineland, Rev. Mod. Phys. **75**, 281 (2003); L. M. K. Vandersypen and I.L Chuang, Rev. Mod. Phys. **76**, 1037 (2005); K. Singer, U. Poschinger, M. Murphy, P. Ivanov, F. Ziesel, T. Calarco, F. Schmidt-Kaler, Rev. Mod. Phys. **82**, 2609 (2010); H. Haffner, C. F. Roose, R. Blatt, Phys. Rep. **469**, 155 (2008); L.-M. Duan, C. Monroe, Rev. Mod. Phys. **82**, 1209 (2010); J.-W. Pan, Z.-B. Chen, C.-Y. Lu, H. Weinfurter, A. Zeilinger, M. Żukowski, Rev. Mod. Phys. **84**, 777 (2012), and references therein.

[22] L. Henderson and V. Vedral, Phys. Rev. Lett. **84**, 2263 (2000); M. B. Plenio and V. Vedral, J. Phys. A: Math. Gen. **34**, 6997 (2001); V. Vedral, Rev. Mod. Phys. **74**, 197 (2002).

[23] D. A. Meyer and N. R. Wallach, J. Math. Phys. **43**, 4273 (2002).

[24] A. Osterloh and J. Siewert, Phys. Rev. A **72**, 012337 (2005); Int. J. Quant. Inf. **04**, 531 (2006); D. Ž. DJoković and A. Osterloh, J. Math. Phys. **50**, 033509 (2009); L. E. Buchholz, T. Moroder, O. Gühne, arXiv:1412.7471 [quant-ph] (2014).

[25] A. Shimony, Ann. NY Acad. Sci. **755**, 675 (1995); H. Barnum and N. Linden, J. Phys. A **34**, 6787 (2001); T. -C. Wei, and P. M. Goldbart, Phys. Rev. A **68**, 042307 (2003); T. -C. Wei, M. Ericsson, P. M. Goldbart, and W. J. Munro, Quantum Inform. Compu. **4**, 252 (2004); D. Cavalcanti, Phys. Rev. A **73**, 044302 (2006),

[26] M. Blasone, F. Dell'Anno, S. DeSiena, and F. Illuminati, Phys. Rev. A **77**, 062304 (2008).

[27] A. Sen(De) and U. Sen, Phys. Rev. A **81**, 012308 (2010).

[28] J. Eisert and D. Gross, in Lectures on Quantum Information, edited by D. Bruss and G. Leuchs (Wiley-VCH, Weinheim, 2006).

[29] V. Coffman, J. Kundu, and W. K. Wootters, Phys. Rev. A **61**, 052306 (2000).

[30] R. Prabhu, A. K. Pati, A. Sen(De), and U. Sen, Phys. Rev. A **86**, 052337 (2012).

[31] A. Sen(De) and U. Sen, Phys. Rev. A **85**, 052103 (2012); M. N. Bera, R. Prabhu, A. Sen(De), and U. Sen, Phys. Rev. A **86**, 012319 (2012).

[32] D. M. Greenberger, M. A. Horne, and A. Zeilinger, in Bell's Theorem, Quantum Theory, and Conceptions of the Universe, ed. M. Kafatos (Kluwer Academic, Dordrecht, The Netherlands, 1989).

[33] D. P. DiVincenzo, C. A. Fuchs, H. Mabuchi, J. A. Smolin, A. Thapliyal, and A. Uhlmann, arXiv:quant-ph/9803033v1 (1998); T. Laustsen, F. Verstraete, and S. J. van Enk, Quantum Inf. Comput. **3**, 64 (2003); G. Gour, Phys. Rev. A **72**, 042318 (2005); J. A. Smolin, F. Verstraete, and A. Winter, Phys. Rev. A **72**, 052317 (2005); G. Gour, D. A. Meyer, and B. C. Sanders, Phys. Rev. A **72**, 042329 (2005); G. Gour, and R. W. Spekkens, Phys. Rev. A **73**, 062331 (2006); Z.-G. Li, S.-M. Fei, S. Albeverio, and W. M. Liu, Phys. Rev. A **80**, 034301 (2009).

[34] S. Popescu and D. Rohrlich, Phys. Lett. A **166**, 293 (1992).

[35] A. Sen(De), U. Sen, M. Wiesniak, D. Kaszlikowski, and M. Żukowski, Phys. Rev. A, **68**, 062306 (2003).

[36] F. Verstraete, M. Popp, and J. I. Cirac, Phys. Rev. Lett. **92**, 027901 (2004); M. Popp, F. Verstraete, M. A. Martín-Delgado, and J. I. Cirac, Phys. Rev. A **71**, 042306 (2005).

[37] A. Zeilinger, M. A. Horne, and D. M. Greenberger, in Proceedings of Squeezed States and Quantum Uncertainty, edited by D. Han, Y. S. Kim, and W. W. Zachary, NASA Conf. Publ. **3135**, 73 (1992).

[38] W. Dür, G. Vidal, J. I. Cirac, Phys. Rev. A **62**, 062314 (2000).

[39] R. Dicke, Phys. Rev. **93**, 99 (1954).

[40] G. Tóth, J. Opt. Soc. Am. B **24**, 275 (2007); S. Hartmann, arXiv:1201.1732 [quant-ph] (2012); M. Bergmann and O. Gühne, J. Phys. A: Math. Theor. **46**, 385304 (2013); B. Lücke, J. Peise, G. Vitagliano, J. Arlt, L. Santos, G. Tóth, and C. Klempt, Phys. Rev. Lett. **112**, 155304 (2014); A. Kumar, H. S. Dhar, R. Prabhu, A. Sen(De), and U. Sen, arXiv:1505.01748 [quant-ph] (2015).

[41] M. J. Holland and K. Burnett, Phys. Rev. Lett. **71**, 1355 (1993); R. Krischek, C. Schwemmer, W. Wieczorek, H. Weinfurter, P. Hyllus, L. Pezzé, and A. Smerzi, Phys. Rev. Lett. **107**, 080504 (2011); G. Tóth, Phys. Rev. A **85**, 022322 (2012); P. Hyllus, W. Laskowski, R. Krischek, C. Schwemmer, W. Wieczorek, H. Weinfurter, L. Pezz, and A. Smerzi, Phys. Rev. A **85**, 022321 (2012); A. Chiuri, C. Greganti, M. Paternostro, G. Vallone, and P. Mataloni, Phys. Rev. Lett. **109**, 173604 (2012); A. Noguchi, K. Toyoda, and S. Urabe, Phys. Rev. Lett. **109**, 260502 (2012).

[42] B. K. Chakrabarti, A. Dutta, and P. Sen, Quantum Ising Phases and Transitions in Transverse Ising Models (Springer, Heidelberg, 1996); S. Sachdev, Quantum Phase Transitions (Cambridge University Press, Cambridge, 2011); S. Suzuki, J. -I. Inou, B. K. Chakrabarti, Quantum Ising Phases and Transitions in Transverse Ising Models (Springer, Heidelberg, 2013).

[43] E. Lieb, T. Schultz, and D. Mattis, Ann. Phys. **16**, 407 (1961); E. Barouch, B.M. McCoy, and M. Dresden, Phys. Rev. **2**, 1075 (1970); P. Pfeuty, Ann. Phys. **57**, 79 (1970); E. Barouch and B.M. McCoy, Phys. Rev. **3**, 786 (1971).

[44] H. A. Bethe, Z. Phys. **71**, 205 (1931).

[45] C. N. Yang and C. P. Yang, Phys. Rev. **150**, 321 (1966); C. N. Yang and C. P. Yang, Phys. Rev. **150**, 327 (1966); A. Langari, Phys. Rev. B **58**, 14467 (1998); D. V. Dmitriev, V. Y. Krivnov, A. A. Ovchinnikov, and A. Langari, J. Exp. Theor. Phys. **95**, 538 (2002); S Mahdavifar, J. Phys.: Condens. Matter **19** 406222 (2007).

[46] H.-J. Mikeska, A. K. Kolezhuk, Lecture Notes in Physics **645**, 1 (2004).

[47] M. Takahashi, Thermodynamics of One-Dimensional Solvable Models (Cambridge University Press, Cambridge, 1999).

[48] F. Vestraete, J. Dehaene, B. De Moor, and H. Verschelde, Phys. Rev. A **65**, 052112 (2002).

[49] C. Eltschka and J. Siewert, J. Phys. A: Math. Theor. **47**, 424005 (2014).

[50] J. I. Latorre, and A. Rierra, J. Phys. A **42**, 504002 (2009); J. Eisert, M. Cramer, and M. B. Plenio, Rev. Mod. Phys. **82**, 277, (2010);

[51] A. Osterloh, L. Amico, G. Falci, and R. Fazio, Nature **416**, 608 (2002); T. Osborne, and M. Nielsen, Phys. Rev. A **66**, 032110 (2002); G. Vidal, J. Latorre, E. Rico, and A. Kitaev, Phys.Rev. Lett. **90**, 227902 (2003).

[52] T. -C, Wei, D. Das, S. Mukhopadyay, S. Vishveshwara, and P. M. Goldbart, Phys. Rev. A **71**, 060305(R) (2005); T. R. de Oliveira, G. Rigolin, and M. C. de Oliveira, Phys. Rev. A **73**, 010305(R) (2006); Phys. Rev. A **74**, 039902 (2006); Phys. Rev. A **75**, 039901 (2007); T. R. de Oliveira, G. Rigolin, M. C. de Oliveira, and E. Miranda, Phys. Rev. Lett. **97**, 170401 (2006); S. M. Giampaolo and B. C. Hiesmayr, Phys. Rev. A **88**, 052305 (2013). Z.-Y. Sun, Y. -Y. Wu, J. Xu, H. -L. Huang, B. -F. Zhan, B. Wang, and C.-B. Duan, Phys. Rev. A **89**, 022101 (2014).

[53] M. Schechter and P. C. E. Stamp, Phys. Rev. B **78**, 054438 (2008), and references therein.

[54] J. Struck, C. Ölschläger, R. Le Targat, P. Soltan-Panahi, A. Eckardt, M. Lewenstein, P. Windpassinger, and K. Sengstock, Science **333**, 996 (2011); J. Simon, W. S. Bakr, R. Ma, M. E. Tai, P. M. Preiss, and M. Greiner, Nature (London) **472**, 307 (2011), and references therein.

[55] J. -J. García-Ripoll and J. I. Cirac, New. J. Phys. **5**, 76 (2003); L. -M. Duan, E. Demler, and M. D. Lukin, Phys. Rev. Lett. **91**, 090402 (2003), and references therein.

[56] D. Leibfried, R. Blatt, C. Monroe, and D. Wineland, Rev. Mod. Phys. **75**, 281 (2003); X. -L. Deng, D. Porras, and J. I. Cirac, Phys. Rev. A **72**, 063407 (2005). H. Häffner, C. Roos, and R.Blatt, Phys. Rep. **469**, 155 (2008); K. Kim, M.-S. Chang, S. Korenblit, R. Islam, E. E. Edwards, J. K. Freericks, G.-D. Lin, L.-M. Duan, and C. Monroe, Nature (London) **465**, 590 (2010); R. Islam, E. E. Edwards, K. Kim, S. Korenblit, C. Noh, H. Carmichael, G.-D. Lin, L.-M. Duan, C.-C. Joseph Wang, J. K. Freericks, and C. Monroe, Nature Commun. **2**, 377 (2011); J. Struck, M. Weinberg, C. Ölschläger, P. Windpassinger, J. Simonet, K. Sengstock, R. Höppner, P. Hauke, A. Eckardt, M. Lewenstein, and L. Mathey, Nature Physics **9**, 738 (2013), and references therein.

[57] L. M. K. Vandersypen and I. L. Chuang. Rev. Mod. Phys. **76**, 1037 (2005); J. Zhang, M.-H. Yung, R. Laflamme, A. Aspuru-Guzik, J. Baugh, Nature Communications **3**, 880 (2012); K. Rama Koteswara Rao, H. Katiyar, T. S. Mahesh, A. Sen(De), U. Sen, and A. Kumar, Phys. Rev. A **88**, 022312 (2013), and references therein.

[58] S. -J. Gu, H. -Q. Lin, and Y. -Q. Li, Phys. Rev. A **68**, 042330 (2003); O. F. Syljuasen, Phys. Rev. A **68**, 060301 (2003).